International Journal of Engineering and Advanced Technology Studies,14 (3),1-32,2026

Print ISSN: 2053-5783(Print)

Online ISSN: 2053-5791(online)

Website: https://www.eajournals.org/

Publication of the European Centre for Research Training and Development -UK

Adsorption Dynamics Studies of *Luffa Cylindrica Seeds* Adsorbent Particulate size and Reactor Properties effects on Effluents Ni^{2+}, Cu^{2+} and Zn^{2+} ions

[1] P. Diagbonya [2]K.K. Dagde; [3]E.O. Ehirim; [4]T.O. Goodhead

[1,2,3, & 4]Department of Chemical/Petrochemical Engineering, River State University, Port Harcourt, Nigeria

doi: https://doi.org/10.37745/ijeats.13/vol14n1132 Published June 27, 2026

Citation: Diagbonya, P., Dagde K.K., Ehirim E.O., Goodhead T.O. (2026) Adsorption Dynamics Studies of Luffa Cylindrica Seeds Adsorbent Particulate size and Reactor Properties effects on Effluents Ni2+, Cu2+ and Zn2+ ions, *International Journal of Engineering and Advanced Technology Studies*,14 (3),1-32

Abstract: Heavy metal pollutants present in our water body pose great threats to environment and human health due to their non-biodegradable and bio-accumulative nature This study explored the use of nitric acid–treated *Luffa cylindrica* seeds adsorbent in removal Ni^{2+}, Zn^{2+}, and Cu^{2+} ions from aqueous stock solutions in a continuous fixed-bed system. The LC adsorbent was produced at a carbonation temperature of 105°C and characterized using the Fourier Transform Infra-Red (FTIR) Scanning Electron Microscope (SEM), and the Brunauer-Emmett-Teller (BET) analytical tool, of which the adsorbent surface area, pore volume, Pore diameter and bulk density were resulted as 23.971m^2/g, 0.011cc/g, 2.402 nm, 0.034 g/cm^3 respectively by the BET analysis, while the active binding sites where identified by FTIR and SEM. Effect of the LC loaded column adsorption height, injection flow rate and adsorbent particulate size on the adsorption efficiency of LC adsorbent was studied at varied injection fluid (SS) flow rate (5, 10, 15mL/min), the adsorbent bed height (5, 7.5, 10cm) and the initial concentration (5, 10, 15mg/L) defining their corresponding impacts on the Stock Solution (SS) pH, TDS, DO, COD, BOD, and the Ni-Cu-Zn ions amounts (ppm) when dynamically conveyed through *Luffa Cylindrica* Medium as a treatment measure. Results achieved form the ST treatment potency assessment of LC medium depicts that on the bases of the column loaded height effects(x), stock solution pH and DO increases proportionally with increase in adsorbent height, while TDS, BOD, COD, and Ni-Cu-Zn ions concentration in the ST reduces dynamically. While on the bases of injected stock solution flow rate (y) it was noticed that the pH and DO increases as the flow rate was within 5 ml/min, before reducing with increase in the fluid flow rate, but TDS, BOD, COD, and Ni-Cu-Zn ions concentration reduces as the stock solution reduces over a flow rate of 5/min after which the properties of water shows lesser recovery nature proportional to increase in the flow rate. The effects of the flow rate on the LC performance tends to be very similar to that experienced for the assessment of the LC adsorbent particulate size (z) effects on the system performance, though the flow rate effects tend to be more effective compared to that caused by increase in the particulate size of adsorbent.

Keywords: Reactor performance, Kinetics, MATLAB, Greenhouse gases (GHGs), Methanol additive, Environmental pollution, Space time, Rate law, Daltons law of partial pressures, Material balance

INTRODUCTION

Solid metals are of tremendous effects to human and microorganisms in the soil, the facilitates rapid environmental pollution such which promotes the reduction of air purity as well as reduces soil potency dynamically (Angon *et al.*, 2024; Perry's and Green, 2007; Ali *et al.*, 2023; Ugi *et al.*, 2023; Wordu *et al.*, 2023). Their presence in the soil reduces the effectiveness of microorganism in fixation of nutrients to plants for efficient agricultural yielding, as well as interferes negatively with chemical reactions in the soil, leading to improper digestion of minerals found within the soil body. Solid heavy metals (like Copper, Nikel, Zink, lead, cadmium, and arsenic) contaminate soil by degrading its physical and chemical properties and

disrupting vital nutrient cycles. They inhibit the growth of beneficial microorganisms, impair nutrient availability, and restrict root development, ultimately reducing soil fertility and causing poor plant yields.

The concentration of these solid metals varies between regions and tends to be of different effects to the soil due to soil type as well, and most times they are been discharged directly or accidentally into the environment by man either as flare gas or effluent (Ugi *et al.,* 2023; Ugi *et al.,* 2025; Igwe *et al.,* 2026b; Ogolo *et al.,* 2026; Lambert *et al.,* 2026; Nathaniel *et al.,* 2026), while few befall on earth source as a result of natural disasters such earthquake and war, but those generated from industrial activities tends more efficient.

Industrialization process materials to finish products, and in most cases generates contaminants as flare gases as well as effluents (wastes water). Petrochemicals and the oil/gas refining industries process materials that consist solid metals in high proportions, and do discharge industrial effluents rich in these metals and her hazardous compounds such as the hydrocarbons into water bodies and the environment, contaminating surface and ground water alike as the atmosphere (Igwe *et al.,* 2026b; Perry's and Green, 2007). Though regulations have been set to control the rate and nature of effluents that are dischargeable by industries, as a measure of safe guiding the environment for humans sake, but most times these regulations are not abided due to poor governance, human ignorance and corruption, hence the heavy metals concentrated effluents are still by possible means finding their ways into the environment, generating serious effects on man's health, promoting metals corrosion (Ita *et al.,* 2026; Obeten *et al.,* 2017; Benedict *et al.*, 2021; Benedict, 2024; Benedict and Mbang, 2019; Ugi *et al.,* 2022; Ugi, 2014; Ugi and Magu, 2017; Ugi *et al.,* 2024; Ugi & Obeten, 2019; Ugi, 2018; Ugi *et al.,* 2016; Ugi & Obeten, 2019; Ugi & Obeten, 2019; Benedict and Fredrick, 2023, Benedict *et al.,* 2022; Ugi *et al.,* 2023; Ugi *et al.,* 2026; Ugi *et al.,* 2021) as well as mitigating soil nutrient over time.

Effluents are wastes water generated from industrial practices as well as from crude oil recovery reservoirs (Igwe *et al.,* 2026b; Sammy *et al.,* 2023), they are environmentally unfriendly and usually been discharged after treatment. But due to insufficient treatment measures the effluents sent into the environment are still identified to be of negative impacts to the soil and man. Solid metals are always regarded not biodegradable (Gupta *et al*, 2009; Abdel-Ghani *et al*, 2009), hence are always advice to be removed or recovered from effluents before been discharged, and on this bases, adsorption has been identified as the most effective means for proper recovery of these metals and other impurities from effluent stream.

Adsorption offers a cleaner technology, free from sludge handling problems and produces a high-quality effluent. Over the last few decades, adsorption has gained importance as an effective purification and separation technique used in water and wastewater treatment. Adsorption is the process by which a solid adsorbent can attach a component dissolved in water to its surface and form an attachment via physical or chemical bonds, thus removing the component from the fluid phase. Adsorption is used extensively in industrial processes for many purposes of separation and purification. The removal of metals, colored and colorless organic pollutants from industrial wastewater are considered an important application of adsorption processes using suitable adsorbents. The most frequently applied adsorbent for the removal of organic pollutants in wastewaters is currently activated carbon. However, activated carbon is an expensive material.

There is growing interest in using low-cost materials for adsorption as alternatives to activated carbons. A wide variety of materials have been used in researches such as peat, lignite, diatomite, dolomite, bone char, zeolites, peanut hulls and a range of other natural materials. Areas in which further developments are

expected, deal with the equilibrium and transport phenomena of fluids in porous materials, with special emphasis on diffusion. In this regard, one of the important elements will require the maintenance of a suitable balance between theoretical and experimental research. One would expect, however, that a wide range of sophisticated modelling and simulation methods will level the enormous gap between microscopic and macroscopic picture scales (Dabrowski, 2001). In the recent past scientists have tried to remove metals and its ions using adsorptive column treatment. Synthetic adsorbents, namely polyacrylonitrile–potassium cobalt hexacyanoferrates and polyacrylonitrile–potassium nickel hexacyanoferrates, were synthesized, and adsorption of cesium was investigated. The effects of liquid flow rate, bed height and presence of other cations on the adsorption of cesium were performed. The bed depth service time (BDST) model and the Thomas model were used to analyze the experimental data, and the model parameters were evaluated (Du *et al*. 2014). Ali had synthesized economical adsorbent, i.e., carbon nanotube using Ni/MgO metal oxide for microwave exposure for thermal disintegration at 550 °C. This microwave-assisted nanotube had undergone column studies for removal of arsenite and arsenate using process variables like initial concentration, flow rate and bed height. The data were analyzed using Thomas and Adam bohart models, and maximum removals were found to be 13.5 and 14.0 mg/g for arsenite and arsenate, respectively (Ali, 2018). Novel 3D yttrium-based graphene oxide–sodium alginate hydrogel was prepared by sol–gel process for removal of fluoride via continuous filtration.

Data were analyzed by Thomas model, and maximum uptake capacity was achieved to be 4.00 mg/g (He *et al*. 2018). Vertical column experiments using sugarcane bagasse were conducted for removal of manganese (II), and the highest removal efficiency was found to be 51.95% (Zaini *et al*. 2018). New chelating cellulose-based adsorbent, i.e., *N*-methyl-d-glucamine (NMDG)-type functional group attached to a novel boron selective chelating fiber, was prepared, characterized and utilized for boron removal. Yoon–Nelson, Thomas and modified dose response model were evaluated using data of various flow rates. Maximum boron adsorption capacity related to Thomas model was obtained up to 22.06 mg/g (Recepoglu *et al*. 2018). Freitas and their co-scientists were experimented for binary adsorption of silver and copper onto bentonite (Verde-lodo clay), in which first flow rate was optimized. Thereafter, effects of initial concentration and molar fraction were investigated using this optimum flow rate (Freitas *et al*. 2018).

Color from real textile effluent was removed in fixed-bed column of modified zeolite (SMZ), in which surface of natural zeolite was modified with a quaternary amine surfactant hexadecyltrimethylammonium bromide (HTAB). Breakthrough curves of different flow rate (0.015–0.075 l/min) and bed height (12.5–50 cm) at original as well as diluted wastewater (ratio of 25, 50 and 75%) were plotted, and breakthrough and exhaust points were calculated for each and every parameter. Also, experiments for regeneration of SMZ using NaCl and NaOH solution were carried out. Data were analyzed by BDST isotherm (Ozdemir *et al*. 2009). Different experiments of packed bed column were demonstrated for adsorption of hexavalent chromium from its synthetic solution (Rangabhashiyam & Selvaraju 2015a) and electroplating industries effluent (Rangabhashiyam *et al.* 2016) using chemically modified swietenia mahagoni shell. Also, caryota urens inflorescence waste biomass was utilized as adsorbent for adsorption of hexavalent chromium (Rangabhashiyam & Selvaraju 2015b).

Activated carbon is the most employed adsorbent for heavy metal removal from aqueous solution and have been well documented in literature (Luqman *et al*, 2010). However, the extensive use of activated carbon for metal removal from industrial effluents is expensive (Babel & Kurniawan, 2003), limiting its large application for wastewater treatment. Therefore, there is a growing interest in finding alternative low-cost adsorbents for metal removal from aqueous solution, such as: microorganisms (Martins *et al*, 2006; Klen

et al, 2007), residuals of agricultural products and its various chemical modifications (Basil *et al*, 2006; Lima *et al*, 2007)

In this study, *Luffa cylindrica* seeds was used as biosorbents and the utility of these very low cost and environmentally friendly plant materials as biosorbents for the removal of divalent cations from aqueous solutions as the cellulose, hemicelluloses, pectin and lignin present in the cell wall are the most important sorption sites (Volesky, 2003; Rowell *et al*, 2002; Mazali & Alves, 2005). *Luffa cylindrica* is derived from the cucumber and marrow family and originates from America (Mazali & Alves, 2005). *Luffa* [*Luffa cylindrica* (L.) Roem syn *L. aegyptiaca* Mill] commonly called sponge gourd, loofa, vegetable sponge, bath sponge or dish cloth gourd, is a member of cucurbitaceous family. The number of species in the genus *Luffa* varies from 5 to 7. Only 2 species *L. cylindrica* and ribbed or ridge gourd [*L. acutangula* (L.) Roxb] are domesticated. *Luffa* is diploid species with 26 chromosomes (2n = 26) and a cross-pollinated crop (Bal *et al*., 2004). Loofa sponge is a lignocellulosic material composed mainly of cellulose, hemicelluloses and lignin (Rowell *et al*., 2002). The fibers are composed of 60% cellulose, 30% hemicelluloses and 10% lignin (Mazali & Alves, 2005). The fruits of *L. cylindrica* are smooth and cylindrical shaped (Mazali & Alves, 2005). One (1) mature Luffa sponge will produce at least 30 seeds. Some will produce many more (Newton, 2006). *L. cylindrica* (Figure 1) has alternate and palmate leaves comprising petiole. The leaf is 13 and 30 cm in length and width respectively and has the acute-end lobe. It is hairless and has serrated edges. The flower of *L. cylindrica* is yellow and blooms on August-September. *L. cylindrica* is monoecious and the inflorescence of the male flower is a raceme and one female flower exists. Its fruit, a gourd, is green and has a large cylinder-like shape. The outside of the fruit has vertical lines and a reticulate develops inside of the flesh. *L. cylindrica* grows about 12 cm long. The stem is green and pentagonal and grows climbing other physical solid (Lee & Yoo, 2006). The loofa sponge is a highly complex macroscopic architectural template, an inexpensive and sustainable resource. The loofa sponge is cultivated, unlike the sponge produced with cellulose that is extracted from trees. The plant is cultivated in many countries, including Brazil, where its cultivation has an increasing economic importance (Mazali & Alves, 2005).

Fig.1: *Luffa cylindrica* Fruit and sponge (Mazali & Alves, 2005)

Fig. 2: *Luffa cylindrica* seeds (Mazali & Alves, 2005)

L. cylindrica is a sub-tropical plant, which requires warm summer temperatures and long frost-free growing season when grown in temperate regions. It is an annual climbing which produces fruit containing fibrous vascular system. It is a summer season vegetable. It is difficult to assign with accuracy the indigenous areas of *Luffa* species. They have a long history of cultivation in the tropical countries of Asia and Africa. Indo-Burma is reported to be the center of diversity for sponge gourd. The main commercial production countries are China, Korea, India, Japan and Central America (Bal *et al*., 2004). Sponge gourd prefers pH of around 6 to 6.8. High level of K and P is recommended for growth. It also grows well in green house and will grow on many soil types but well drained sandy loams are preferred. Seeds need to be germinated at 25ºC and grown on and transplanted when the soil temperature is about 18ºC. Although *L. cylindrica* can be left to grow along the ground, best yields and fruit quality are obtained using a support structure or trellis system (Bal *et al*., 2004). Any constriction will result in deformed fruit. Irrigation is essential for good growth during dry periods but excessive water can result in poor growth and root diseases. Generally, there have been few pest and disease problems of sponge gourd reported in Nepal. Damping off can be a problem with young seedlings if grown in cool wet conditions and fruit rots may cause losses if the fruit are allowed to grow on the ground. Problems with aphids and subsequently viruses have been sometimes reported (Bal *et al*., 2004). Frost kills the plant and it needs 4 to 5 months of growth to produce sponges (Newton *et al*., 2006).

Assessing *L. cylindrica* seed (Figure 2) adsorption efficiency in terms of recovering solid heavy metals from effluent is a significant research that targets cost conservativeness of industrial effluent treatment practice, as providing a low budget adsorbent that can effectively retrieve the active solid metals from the effluent as a function of the reactor's properties and those of the *L. cylindrica adsorbent*

MATERIALS AND METHODS

L. cylindrica (LC) Adsorbent Production and Analyses

The seeds of *L. cylindrica* were gathered into a clean plastic bag. They were dried in the oven at 105^{o}C for 24 hours and afterwards grind with a grinding mill. The grinded seeds were sieved into particle size of 75μm. This was to allow for shorter diffusion path, resulting in a higher rate of biosorption (Adeyinka *et al.*, 2007). Fourier Transform Infrared (FTIR) Analysis was used to detect the surface functional groups associated with the *Luffa cylindrica* seeds in order to deduce the adsorption mechanism on target adsorbates. About 0.25 - 0.50 ml of potassium bromide (KBr) was mixed with 0.1g *Luffa cylindrica* seeds and placed in sample holder of the spectrophotometer (Cary 630 by Agilent Technologies) for recording of spectra. The wave number range of spectra was 350 to 4000 cm^{-1}.

Solid Effluent Solution Preparation and the Adsorption Treatment System Setup

Stock solutions of Nickel, Copper, and Zinc were prepared with distilled water and Nickel (II) tetraoxosulphate (VI), Copper (II) tetraoxosulphate (VI) and Zinc chloride respectively. All working solutions were obtained by diluting the stock solutions with distilled water. The concentration of metal ions in solutions was analyzed by Atomic Absorption Spectrophotometer. A duplicate was analyzed for every sample to track experimental error and show capability of reproducing results (Marshall & Champagne, 1995).

Then a laboratory fixed-bed adsorption column unit used for this study was arranged as seen at Figure 3. The unit consisted of 20mm OD, 500mm long clear acrylic tube with 1.5 mm wall thickness, MEDO XG6 solenoid dosing pump, 1/4 valves, dosing tubes, 2000 cm^3 beaker, 1000 cm^3 measuring cylinder, glass beads, glass wool, Teflon material, bolts, nuts and screws. A 500mm long clear acrylic pipe with 1.5mm wall thickness and 25 mm outer diameter was completed with detachable Teflon ends where inlet and outlet delivery pipes were attached. This is where the adsorption process takes place. The column was packed with glass beads, adsorbent and 5mm thick layers of glass wool in between. During adsorption process, the influent entered the column through the bed of glass beads and the adsorbate in the feed attached itself to the packed bed and got separated from the aqueous solution.

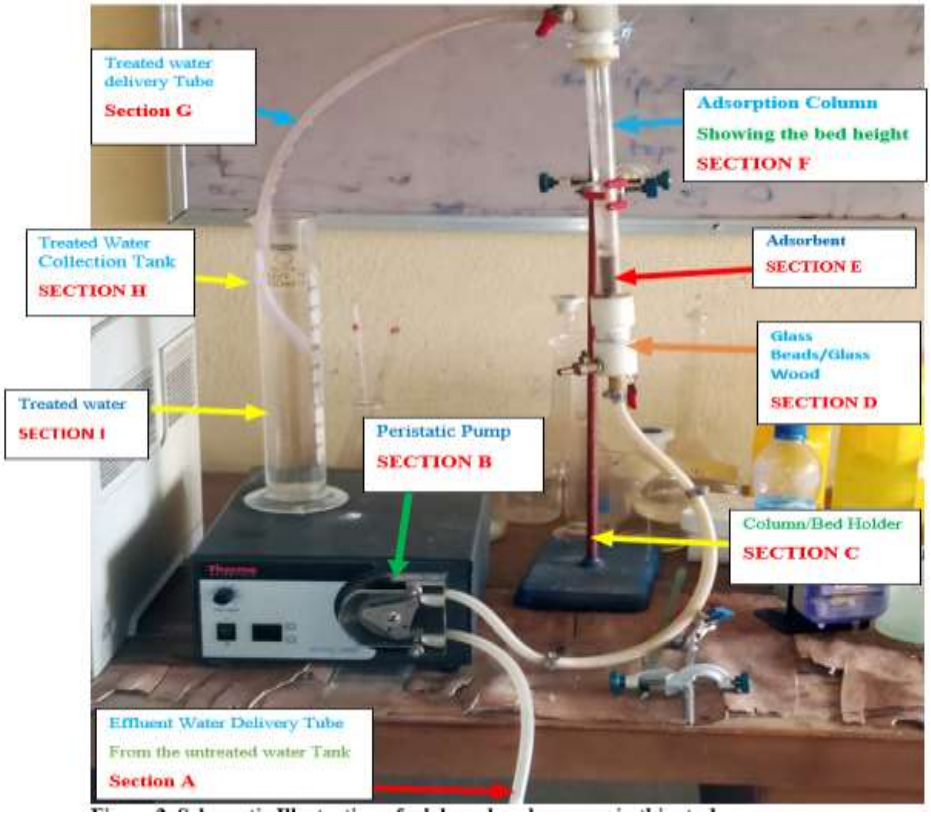

Fig. 3: Schematic Illustration of a lab-scale column use in this study

RESULTS AND DISCUSSION

Results of *Luffa Cylindrica* Seeds Characterization

The characterization results of some physical properties for *Luffa cylindrica* seeds used as biosorbent in this study are given in Table 1 which show the bulk density, surface area, pore volume and pore diameter for the biosorbent. The surface area obtained using the BET method was 23.971m²/g and the Pore diameter, pore volume and bulk density were 2.402 nm, 0.011 cc/g and 0.34g/cm^3 respectively. As observed, the surface area for the seed of *L. cylindrica* was relatively low, with pore diameter value in agreement with those found for typical mesoporous materials (Hamoudi & Kaliaguine, 2013).

Table 1: Physical properties of the *Luffa cylindrica* seeds biosorbent

Surface area - BET (m²/g)	**23.971**
Pore volume (cc/g)	0.011
Pore Diameter (nm)	2.402
Bulk density (g/cm^3)	0.34

Table 2: Elemental compositions of *Luffa cylindrica seeds* obtained from proximate analysis

Element Number	Element Symbol	Element Name	Atomic Conc.	Weight Conc.
6	C	Carbon	78.12	73.13
7	N	Nitrogen	19.61	21.41
19	K	Potassium	0.46	1.39
15	P	Phosphorus	0.47	1.13
12	Mg	Magnesium	0.36	0.68
16	S	Sulfur	0.24	0.60
14	Si	Silicon	0.23	0.50
13	Al	Aluminium	0.19	0.41
17	Cl	Chlorine	0.11	0.30
11	Na	Sodium	0.17	0.30
20	Ca	Calcium	0.05	0.15
22	Ti	Titanium	0.00	0.00
26	Fe	Iron	0.00	0.00

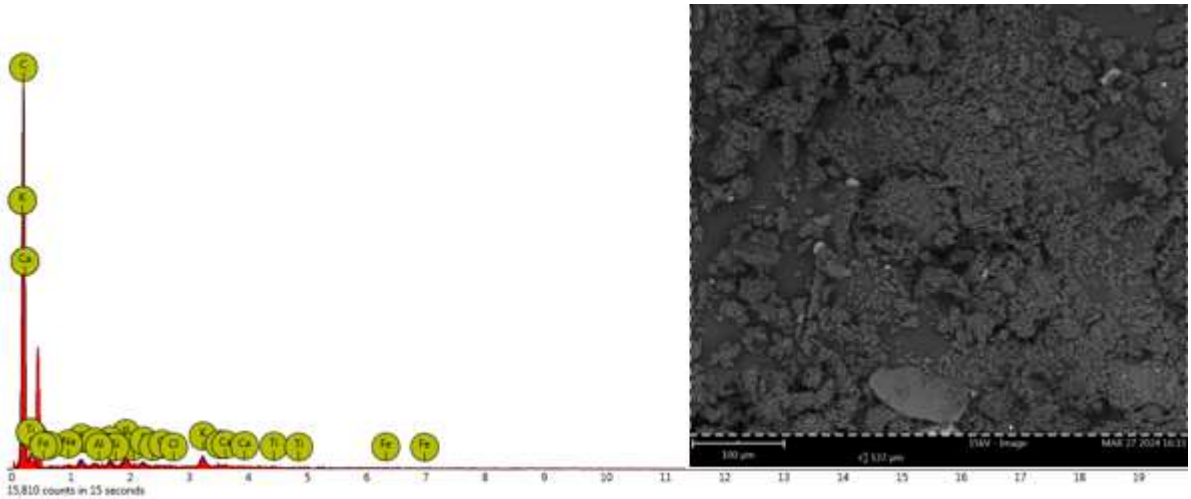

Fig. 4: SEM Scan and plot showing elemental composition of *Luffa cylindrica*

Table 2 gives the elemental composition of *Luffa cylindrica* seeds that were analyzed by means of scanning electron microscopy (SEM) which is also shown in Figure 4. The *Luffa cylindrica seeds* sample showed a very high percentage of carbon followed by nitrogen and potassium.

Scanning electron microscopy (SEM) of the *Luffa cylindrica* seeds biosorbent was taken in order to verify the presence of macropores in the structure of the fiber. In the micrographs presented, Figures 5 when observed showed the fibrous structure of *Luffa cylindrical seeds*, with some fissures and holes, which indicated the presence of macroporous structure. These, should contribute to the diffusion of the Ni (II), Cu (II) and Zn (II) to the *Luffa cylindrica* seeds biosorbent surface (Passos *et al*., 2006; Vaghetti *et al*, 2003; Arenas *et al*., 2004; Passos *et al*., 2008). The small number of macroporous structures is confirmed by the

low surface area (23.971 m²/g), of the biosorbent. As the biosorbent material presents few numbers of macroporous structure, it adsorbed low amount of nitrogen, which led to a low BET surface area (Passos *et al*., 2006; Vaghetti *et al*, 2003; Arenas *et al*., 2004; Passos *et al*., 2008). Therefore, the major contribution of the Ni (II), Cu (II) and Zn (II) uptake can be attributed to micro- and mesoporous structures as shown in Figures 5.

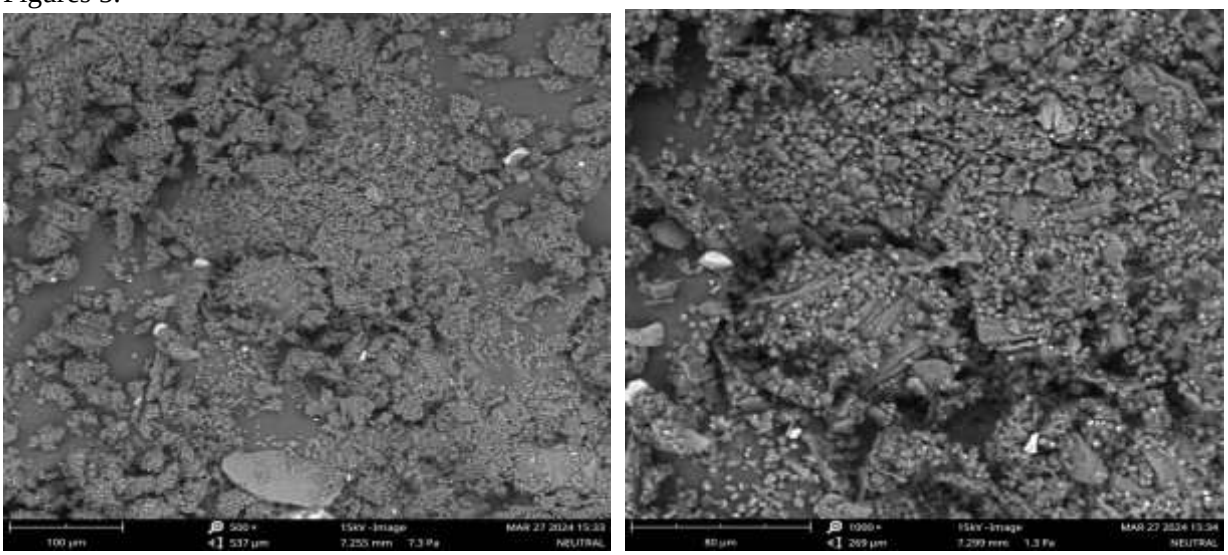

Fig. 5: Scanning electron microscopy of *Luffa cylindrica* seeds biosorbent showing the transversal view of the seed at a magnification of 500 × and at 1000 × (from left to right)

The FTIR analysis of the sample was carried out to find the functional groups present on the surface of the absorbent using the FTIR spectroscope. The FTIR spectrum of the *LC* seeds biosorbent before and after the adsorption is shown in Figures 5-9 respectively. Before the adsorption as shown in Figure 6, there is a clear indication of an intense peak at 3280.1 cm^{-1} attributed to the stretching of the O-H group due to inter-molecular and intra-molecular hydrogen bonding of polymeric compounds such as alcohol and phenols. The peak observed at 3008.0 cm^{-1} was associated with the stretching vibrations of CH bond. The peaks at 15432.1 cm^{-1} corresponded to the C=C stretching which might be attributed to the presence of aromatic or olefinic bands. The intense peak at 2922.2 cm^{-1} corresponds to the C-O stretching of alcohol or carboxylic acid. The band at 1032.5 cm^{-1} indicates the C^{-1} aromatic ring formation, the FTIR spectrum suggested that the surface functional groups containing O_2, which include the carboxyl groups and hydroxyl groups, influences the adsorption characteristics of *LC* seeds biosorbent.

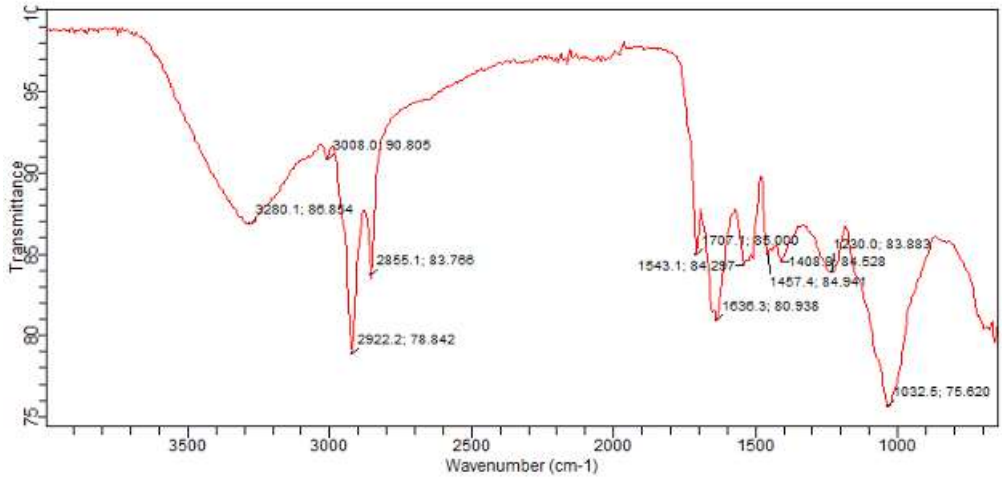

Fig. 6 Figure 4.5: FTIR spectra of *Luffa cylindrica* seeds

After the adsorption of metal ions as shown in Figure 4.6-4.8, the FTIR spectra had shifted slightly after binding with metals. This was due to the participation of these functional groups in the binding of metal ions. The adsorption of the heavy metal ions Zn (II), Cu (II) and Ni (II) caused the intensity of the broad bands at 2918.5 cm $^{-1}$ for CH bond vibration stretching, 2847.7 cm^{-1} for C=C stretching and 1032.5 cm^{-1} for C−O stretching of alcohol to increase, This proves that the heavy metal ions bonded with oxygen containing functionalities on the surface of *luffa cylindrica* seeds biosorbent (Eletta *et al.*2019; Ullah *et al.* 2020). A similar result was also reported for adsorption of copper (II) from aqueous solution using *luffa cylindrica* seeds as adsorbents (Oboh *et al.,* 2018; Okolo *et al.* 2020) and adsorption of copper (II) from wastewater using *luffa cylindrica* adsorbent (Nwosu-obieogu *et al.* 2021).

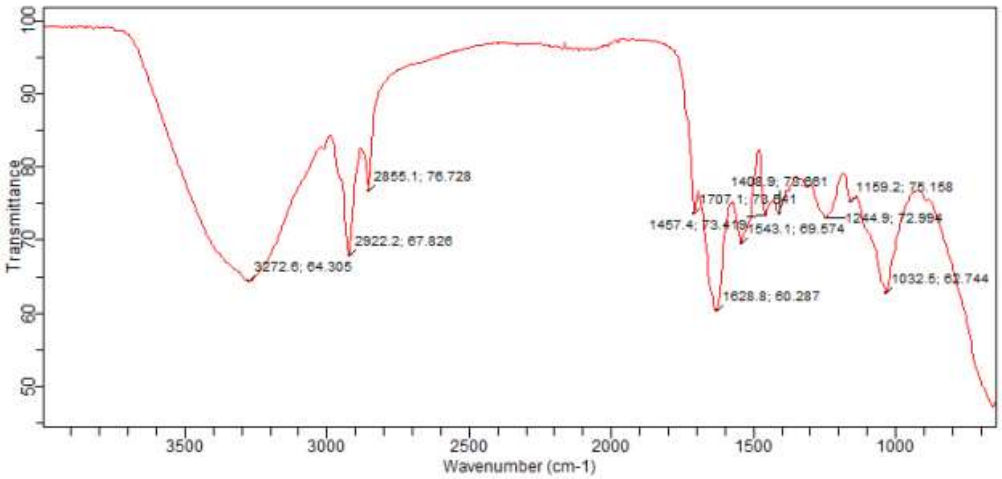

Fig. 7 Figure 4.6: FTIR spectra of *Luffa cylindrica seeds* after Ni (II) ion adsorption

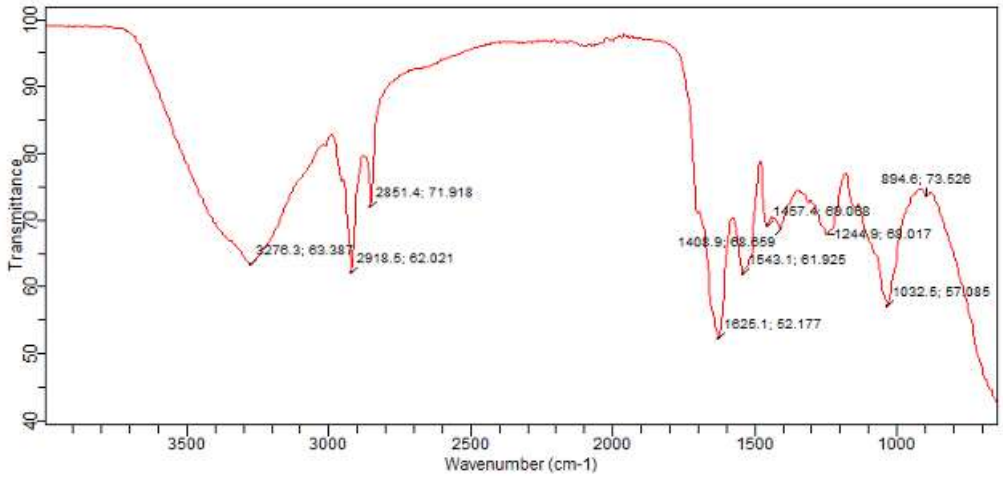

Fig. 8 Figure 4.7: FTIR spectra of *Luffa cylindrical seeds* after Cu (II) ion adsorption

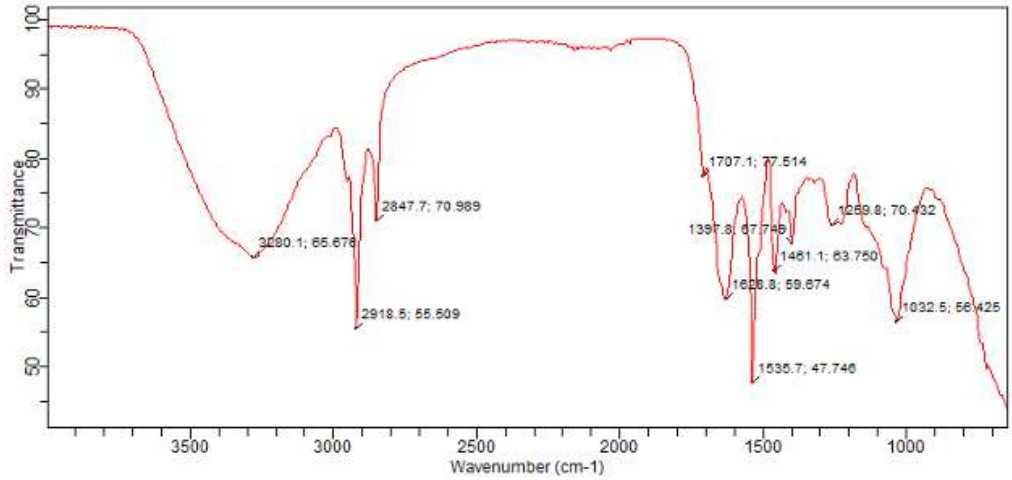

Fig. 9 Figure 4.8: FTIR spectra of *Luffa cylindrical seeds* after Zn (II) ion adsorption

The pore diameter and pore volume of *Luffa cylindrica* seeds used for this study was determined by BET methods with the aid of Quantachrome Instruments version 11.03. The average pore diameter and pore volume of the *Luffa cylindrica* seeds bioadsorbent were deduced from Figure 10. The average pore diameter of *Luffa cylindrica* seeds biosorbent was 2.402 nm while its average pore volume was 0.011 cc/g.

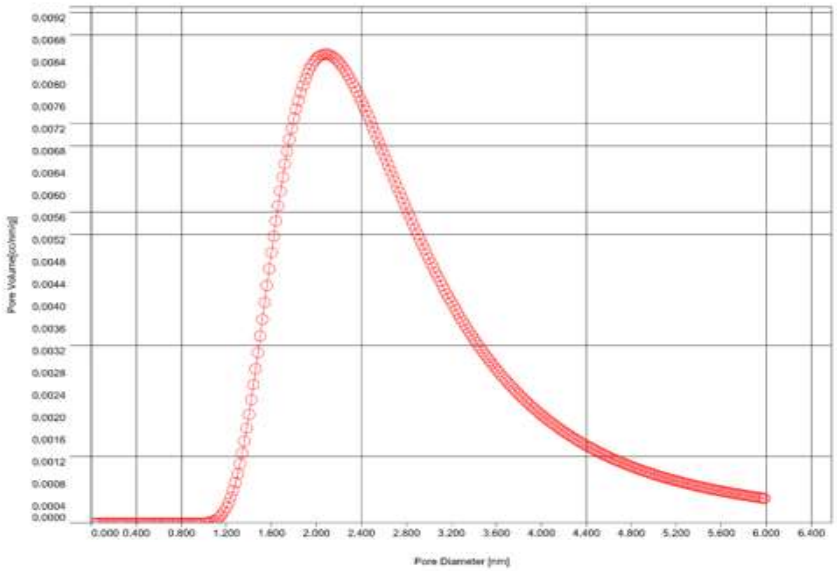

Fig. 10 Figure 4.9: Pore size distribution of the *luffa cylindrica* seed obtained from BET analysis

Results of *Luffa Cylindrica* Seeds Adsorbent Performance in Effluent Metals Recovery as Function of Reactor Properties

Ni-Cu-Zn Produced Stock Effluent Physicochemical status

Stock solutions of Nickel, Copper, and Zinc were prepared with distilled water and Nickel (II) tetraoxosulphate (VI), Copper (II) tetraoxosulphate (VI) and Zinc chloride respectively. All working solutions were obtained by diluting the stock solutions with distilled water (Marshall & Champagne, 1995). The produced stock solution properties after been prepared result showed in Table 3

Table 3 Physicochemical status of stock solution

Physicochemical	**Untreated Stock Solution**		
	Co-10g/l	**Co-20g/l**	**Co-30g/l**
pH	4.6	3.4	2.9
TDS (mg/l)	16342	22331	31322
DO (mg/l)	0.063	0.011	0.009
BOD (mg/l)	6778	12052	17033
EC (S/m)	1333	3432	5224
COD (mg/l)	11757	17990	23609
Ni^{2+} (mg/l)	943	1178	1626
Cu^{2+} (mg/l)	1543	1845	2467
Zn^{2+} (mg/l)	1334	1534	2017

Stock Effluent Metallic and Physicochemical Treatment Efficiency of *Luffa Cylindrica* Seed Adsorbent.

A unique study approach was employed and the outcome sectioned in three stationarity levels, with each stationarity level defining the behavioral nature of stock solution physicochemical properties over changes in the biosorbent particulate size, effluent injection fluid flow rate and the packed bed reactor height, as a

function of the stock solution contaminants. So, the stationarity level one (1) is of the 10g/l contaminant concentration value, while that of level two (2) is of 20g/l contaminant concentration value and finally the level three (3) consist 30g/l contaminant concentration value. Using the produced activated carbon of *Luffa Cylindrica (LC)* Seed in treatment of the Ni-Cu-Zn Stock solution (which was prepared from the combination of Nickel (II) tetraoxosulphate (VI), Copper (II) tetraoxosulphate (VI) and Zinc chloride, in determining the treatment and metal retrieving efficiency of the *Luffa Cylindrica* adsorbent, especially in the case of Ni^{2+}, Cu^{2+} and Zn^{2+} ions retrieval efficiency, and the stock effluent physicochemical variation at variant loaded mass ratio, injection flow rate and particulate size, are been discussed vividly following the experimental results presented as Table 4, Table 5 and Table 6, of which the result shows that increase in the concentration of Nickel (II) tetraoxosulphate (VI), Copper (II) tetraoxosulphate (VI) and Zinc chloride in the solution promotes increase in the level of deviation of the physiochemical properties of the effluent from WHO standard set point.

Effect of Column Adsorption Height on Stock Solution Physicochemical and metal concentration in Aqueous Solution using activated *Luffa cylindrica seeds*.

In this section, the column height of 5cm, 7.5cm and 10cm are considered as the loading factors of the adsorption reactor, operated with different stock solutions concentration using 75µm particulate size *Luffa Cylindrica* biosorbent, subject to 5 mL/min fluid injection flow rate. The effects of the column system on the stock solution physicochemical nature of the effluent and on the metals composite are recorded and discussed vividly for assessment of *Luffa Cylindrica* performance as function of the *Luffa Cylindrica* column height.

Table 4: Physicochemical and metallic adoption efficiency of *Luffa Cylindrica* Seed ACs at different reactor bed height (x)

Physicochemical	Untreated Stock Solution			Treated @ 5cm Biosorbent			Treated @ 7.5 cm Biosorbent			Treated @ 10cm Biosorbent		
	Co-10g/l	Co-20g/l	Co-30g/l	Cfx1-10g/l	Cfx1-20g/l	Cfx1-30g/l	Cfx2-10g/l	Cfx2-20g/l	Cfx2-30g/l	Cfx3-10g/l	Cfx3-20g/l	Cfx3-30g/l
pH	4.6	3.4	2.9	5.3	4.0	3.4	6.2	4.3	3.9	6.9	5.1	4.5
TDS (mg/l)	16342	22331	31322	14704	20188	28431	12921	19891	26866	6705	16086	24033
DO (mg/l)	0.063	0.011	0.009	0.168	0.072	0.019	0.9032	0.186	0.023	1.8912	0.893	0.109
BOD (mg/l)	6778	12052	17033	4535	10706	15996	2034	8086	12672	623	5766	8345
EC (S/m)	1333	3432	5224	701	3020	4357	398	2781	4064	21	2144	3873
COD (mg/l)	11757	17990	23609	8586	14753	21234	4996	12897	17680	1218	9508	11289
Ni^{2+} (mg/l)	943	1178	1626	614	954	1554	297	834	1223	64	585	989
Cu^{2+} (mg/l)	1543	1845	2467	1020	1597	2153	721	1244	1874	435	921	1504
Zn^{2+} (mg/l)	1334	1534	2017	934	1225	1886	498	908	1435	78	478	1154

Effect of Column Adsorption Height on Stock Solution pH in LC medium.

As of the pH of the stock solution, studied at different loading height (cm) of the reactor with *Luffer Cylindrica* as biosorbent was initially identified that 10 g/l contaminated stock solution was of pH value

4.6, while 20 g/l and 30 g/l were of pH 3.4 and 2.9 respective which defines the solution pH to increase with respect to increase of the Nickel (II) tetraoxosulphate (VI), Copper (II) tetraoxosulphate (VI) and Zinc chloride in water. This pH as seen as Figure 4.10 increases with increase in the adsorbent height but reduces with increase in the stock solution contaminant concentration. Standing on the bases of 10g/l concentrated contaminant level of the stock solution, the solution pH decreases from 4.6 to 5.3, 4.9 and 4.7 as the solution was allowed to transport through *Luffer Cylindrica* biosorbent medium of height 5cm, 7.5cm and 10cm. While on the contaminant concentration bases of 20g/l, the pH depletes from 3.4 to 4.0, 4.3 and 5.1 over same increase in the *Luffer Cylindrica* medium loading reactor height. Then at 30g/l concentration bases of the stock solution, the pH decreases from 2.9 to 3.4, 3.9 and 4.5 over same increase in the *Luffer Cylindrica* medium loading height of 5cm, 7.5cm and 10cm respectively as seen at Figure 4.11.

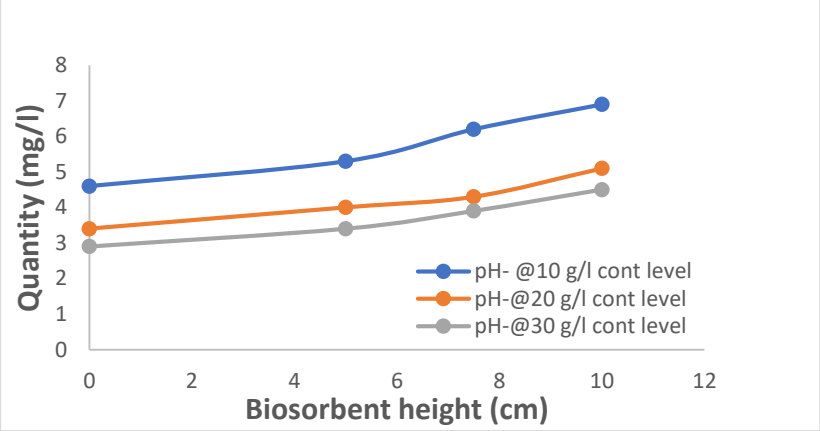

Fig. 11 Figure 4.10: pH behavior at different loaded adsorbent height

The increase in the pH of the stock solution as seen at Figure 4.10 reduces the acidity of the effluent and conveys the water to it WHO standard level, of which using *Luffer Cylindrica* height of 10cm promotes the pH to increase from 6.9 for a 10g/l contaminated stock solution

Effect of Column Adsorption Height on Stock Solution TDS in LC medium.

As for the total dissolved solids (TDS), presented as Figure 4.12, shows that the TDS reduces with increase in the adsorbent loaded height in the reactor, such that 10g/l contaminant concentrated stock solution whose TDS was identified as 16342, was noticed to have been reducing to 14704 mg/l, 12921 mg/l and 6705 mg/l when passed through the *Luffer Cylindrica* medium in a packed bed / column reactor of *Luffer Cylindrica* loading height of 5cm, 7.5cm and 10cm respectively. Also, the 20g/l concentrated stock solution experience a reduction in its TDS value from 22331 mg/l to 20188 mg/l, 19891 mg/l, and 16086 mg/l, so applicable to the 30g/l concentrated stock solution sample as presented at Figure 4.12 which proves *Luffer Cylindrica* as effective medium for TDS reduction of water when conveyed through its adsorbent medium.

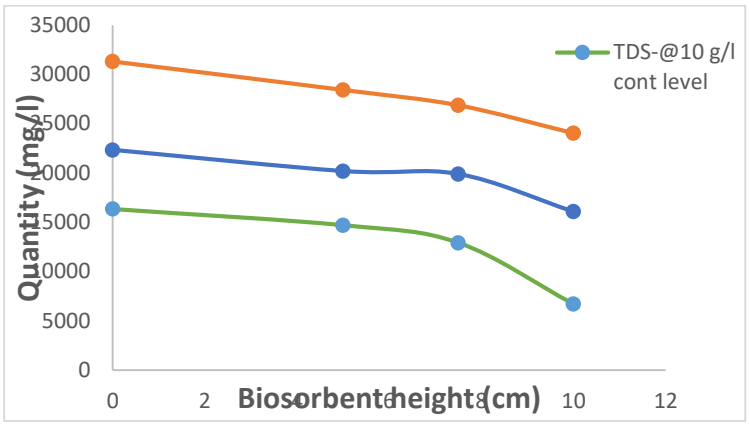

Fig. 12 Figure 4.11: Stock solution TDS behavior over LC Medium height

The 30g/l contaminated stock solution shows the steadiest and linearized form of TDS depletion over increase in the adsorbent height which depicts that higher adsorbent height is more recommended for treatment of a high TDS solution such as the Ni-Cu-Zn solution

Effect of Column Adsorption Height on Stock Solution DO in LC medium.

The dissolve oxygen (DO) level of the stock solution which was identified to be 0.063 mg/l, 0.011 mg/l, and 0.009 mg/l for 10 g/l, 20 g/l and 30 g/l respective Ni-Cu-Zn concentrated metals fluid was identified to have an increasing DO value proportional to increase in the column loading factor of *Luffer Cylindrica*, but also reduces in is remediating nature with increase in the contaminants concentration, such that 0.063 mg/l DO of the 10mg/l effluent increases to 0.168 mg/l, 0.9032mg/l and 1.8912mg/l as the solution is been passed through 5cm, 7.5cm and 10cm *Luffer Cylindrica* medium in column reactor respectively as presented at Figure 4.13, while the 20g/l contaminated stock solution increases in its DO value from 0.011 mg/l to 0.072 mg/l, 0.186 mg/l and 0.893 mg/l lesser than that attained using same loaded *Luffer Cylindrica* medium but with lower stock solution concentration. The 30g/l concentrated stock solution shows a lower DO elevation rate such that increases from 0.009 mg/l to 0.019 mg/l, 0.023 mg/l and 0.109 mg/l

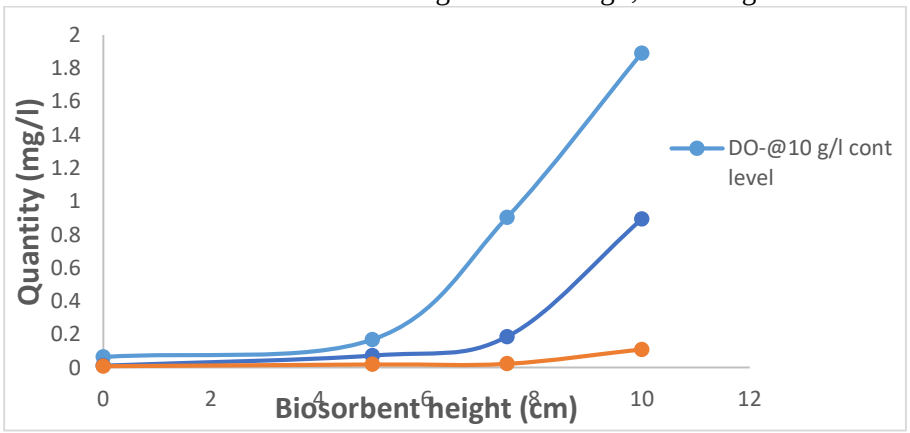

Fig. 13 Figure 4.12: Stock solution DO behavior over LC Medium height

As seen at Figure 13, the stock solution with the lowest Ni-Cu-Zn contaminant of (10g/l concentration) experiences a faster increase in the solution DO value compared to the 20mg/l and 30mg/l stock solutions. The 10 g/l effluent stream starts experiencing DO improvement as earlier than 5cm loaded factor while the

20 g/l kicks up its DO reducibility at about 2.3cm of the *Luffer Cylindrica* loaded height of the reactor, while the 30mg/l commence its DO reduction as from the 5.3cm loaded height as seen at Figure 13.

Effect of Column Height on Stock Solution COD and BOD in LC Medium.

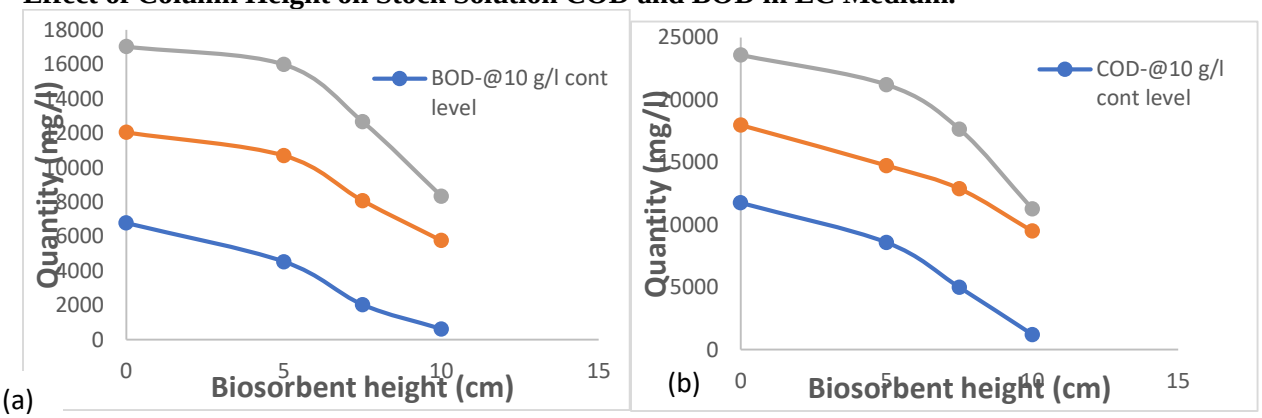

Fig. 14 Figure 4.13 (a & b): Stock solution COD and BOD behavior over LC Medium height

The biological oxygen demand (BOD) of the stock solution as well as the chemical oxygen demand (COD) were assessed and identified as to behave opposite to the behavioral nature of DO of the effluent, such that DO of the effluent was identified to increase with increase in the *Luffa Cylindrica* medium height in the reactor, while the COD and BOD reduces progressively, still defining a good quality of the *Luffa Cylindra* adsorbent used in treatment of contaminated water. Between the BOD and COD, it can be seen at Figure 14 that the COD depletes more simultaneously than the effluent BOD as the loading factor of the reactor increases from 5cm to 10cm. After 7.5cm medium height, BOD shows a slower reduction rate despite the concentration of the stock effluent, these depicts that between the two variables or water properties, COD is easily remediated than BOD in a system of *Luffa Cylindrica* adsorbent

Effect of Column Adsorption Height on Stock Solution Ni, Cu and Zn in LC

In assessment of the Ni-Cu-Zn metal ions behavior in the system has been treated using different *L.Cylindria* medium column height, it was identified that the metals concentration in the stock solution reduces at different rate, as function of the metals diffusion nature and the reactor properties. Cu^{2+} ions prove to be more diffusion efficiency with LC as it shows a steady and faster depletion or reduction from the solution, such that 1543 mg/l Cu^{2+} ion which was initially present in the solution reduces to 1020 mg/l, 721 mg/l and 435 mg/l over transport of the fluid to LC medium of column height 5cm, 7.5cm, 10cm respectively based on 10 g/l contaminant stock solution level. Still from Figure 15 it can be seen that the stock solution or effluent with high Cu^{2+}, Zn^{2+}, and Ni^{2+} ions show a reduces tends to depletes vigorously than that with lower concentration as seen at Figure 15 still with Cu^{2+} ions been more stable adsorbed at a measure proportional to increase in the column height. Also, the Ni-Cu-Zn metals adsorbent adsorption efficiency reduces with increase in the stock solution concentration across the group but increases with increase in the loading factor of the reactor. This phenomenon is also applicable to the physicochemical properties of the effluent stock solution.

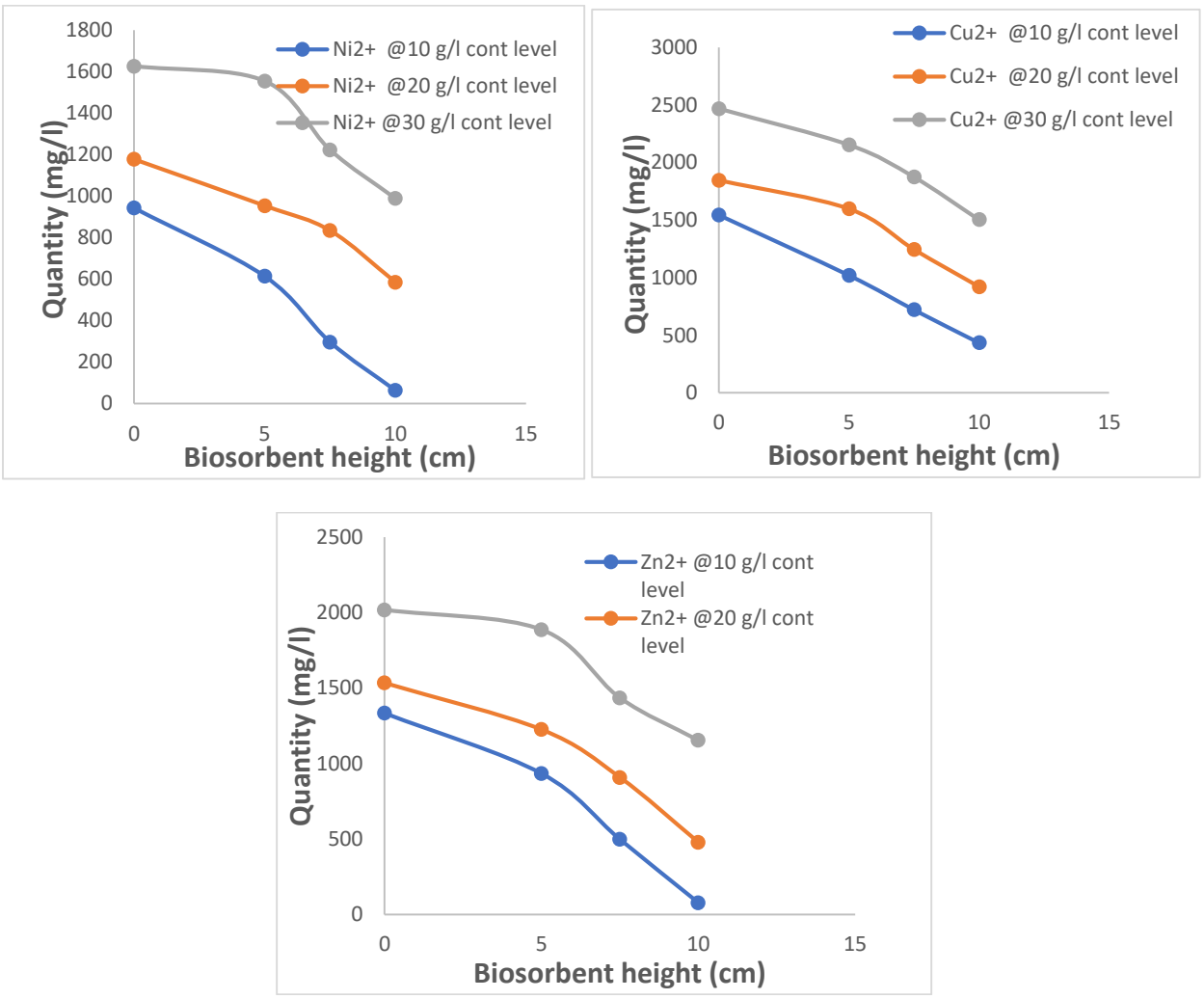

Fig. 15 (a, b and c): Stock solution COD and BOD behavior over LC Medium height

Effect of Fluid Injection Flow Rate on Stock Solution Physicochemical and metal concentration in Aqueous Solution using activated *Luffa cylindrica seeds*.

Fluid flow rate has great influence on the performance of the packed bed reactor as well as the adsorbent used, as it determines the fluidization nature of the reactor, and such alters the degree of adsorptivity as well as the rate of deviation of the physicochemical properties of the injected fluid. So, on the bases of flow rate, this section coveys results of different rates stock solution injection (at 5 mL/min, 10 mL/min and 15 mL/min) through a 5cm loaded height LC adsorbent of 75µm.

Table 5: Physicochemical ad metallic adoption efficiency of *Luffa Cylindrica* Seed ACs at different Stock solution flow rate into reactor (y)

Physicochemical	Untreated Stock Solution			Treated @ 5 mL/min Biosorbent			Treated @ 10 mL/min Biosorbent			Treated @ 15 mL/min Biosorbent		
	Co-10g/l	Co-20g/l	Co-30g/l	Cfy1-10g/l	Cfy1-20g/l	Cfy1-30g/l	Cfy2-10g/l	Cfy2-20g/l	Cfy2-30g/l	Cfy3-10g/l	Cfy3-20g/l	Cfy3-30g/l
pH	4.6	3.4	2.9	5.3	4.0	3.4	4.7	3.6	3.0	4.6	3.5	3.0
TDS (mg/l)	16342	22331	31322	14704	20188	28431	15426	20931	29004	16045	21402	29661
DO (mg/l)	0.063	0.011	0.009	0.168	0.072	0.019	0.153	0.046	0.014	0.148	0.035	0.010
BOD (mg/l)	6778	12052	17033	4535	10706	15996	4911	11025	16002	4209	11474	16872
EC (S/m)	1333	3432	5224	701	3020	4357	812	3109	4503	911	3281	4720
COD (mg/l)	11757	17990	23609	8586	14753	21234	9043	14912	21786	10231	15408	21995
Ni^{2+} (mg/l)	943	1178	1626	614	954	1554	689	984	1577	722	1022	1610
Cu^{2+} (mg/l)	1543	1845	2467	1020	1597	2153	1087	1702	2206	1123	1783	2269
Zn^{2+} (mg/l)	1334	1534	2017	934	1225	1886	981	1288	1921	1009	1343	1940

Effect of Column Injection Flow Rate on Stock Solution pH in LC medium.

The pH of the stock solution as assessed on the bases of the fluid injection flow rate through a 75µm micro particulates LC medium of 5cm bed height was able to show a sudden fall in the elevated pH value proportional to increase in the fluid injection flow rate. The pH of 4.6 which was determined for a 10 g/l concentrated stock solution rises to 5.3 at a 5ml/min injection flow rate then after drops to 4.7 and 4.6 as the flow rate increases to 10ml/min and 15ml/min respectively. Similar experience is recorded for 20g/l concentrated stock solution as well as 30 g/l concentrated effluent as seen at Figure 16 with 3.4 pH rising to 3.5 then starts falling to 4.0 and 3.6 for 20g/l solution, and 2.9 pH of 30g/l concentrated stock solution rises to 3.4 before respective falling to 3.0 and 3.0 for injection flow rate increase from 5ml/min to 10ml/min and 15ml/min respectively. This act defines fluidization of the bed as a phenomenon that reduce the LC efficiency in acidic / alkaline balance of a fluid when used as adsorbent.

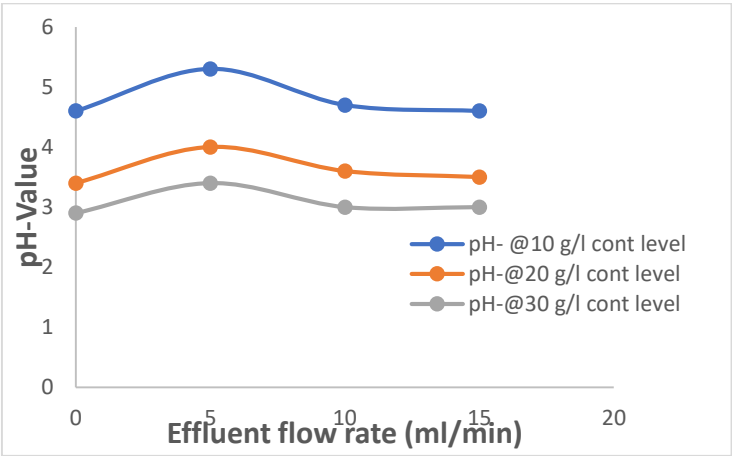

Fig. 16: Stock Solution pH behavior over Flow Rate through LC Medium

The pH reducing effects which has been identifies to be proportional to increase in the injection fluid rate is also identified to be subject to the fluid concentration, such that fluid or stock solution with higher

contaminant concentration will face lesser fluidization effect over increase in bed fluidization and particulates distortion.

Effect of Column Injection Flow Rate on Stock Solution TDS in LC medium.

Also, the TDS of the injected fluid when assessed on the bases of the difference in the injection fluid rate proves to be affected by increase in the fluid injection rate, such that increase in the fluid rate promotes the fall in the rate of reduction of the fluid TDS, hence causing sudden rise in the fluid or stock solution TDS as seen at Figure 17, which promotes the contaminant ratio or concentration in the stock solution over time.

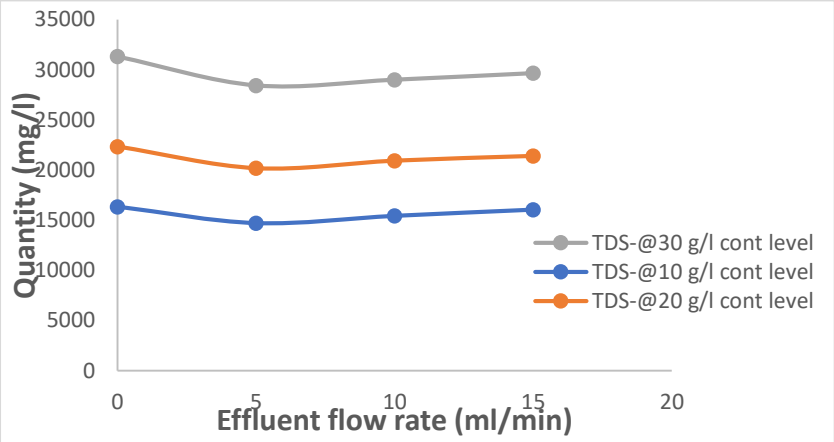

Fig. 17: Stock Solution TDS behavior over Flow Rate through LC Medium

TDS of a 10g/l concentrated stock solution shows a sudden rise from 16342 mg/l to 14704 mg/l as the injection flow rate was set to operate at 5ml/min but start decreasing very gradually as the injection rate increases above 5ml/min to 10ml/min and 15ml/min respectively as 15426mg/l and 16045 mg/l, as well as sudden rise was identified for a 20g/l concentrated effluent and that of 30g/l concentration as the flow rate exceeds 5ml/min to 10ml/min and 15ml/min as seen at Figure 17. This result depicts that TDS of a fluid experience slight increase as the injected fluid rate is been increase as well as when the bed fluidization state increases from normality point. Still from the result it can be concluded that fluid moving with high injection flow rate are liable to experience no change in TDS level as well as pH level over time.

Effect of Column Injection Flow Rate on Stock Solution DO in LC medium.

The dissolved oxygen (DO) of the system also shows that it as subject to the column bed state of operations such that increased injection pressure of the fluid stands to reduce the growth of the effluent or stock solution DO as a sudden rise at 5ml/min operations as seen at Figure 18.

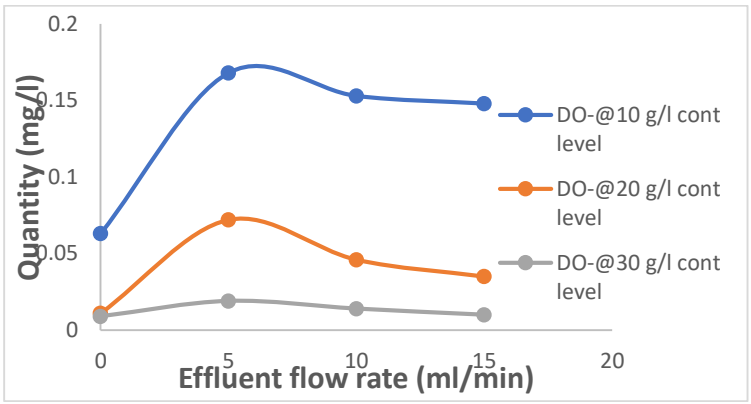

Fig. 18: Stock Solution DO behavior over Flow Rate through LC Medium

The DO shows a sloppy fall after 6ml/min injection which is more withstanding compared to pH and TDS whose fall was experienced at injection rate lesser than 5ml/min, depicting a higher resistivity of DO to sudden increase in column injection rate.

3.1.1.1.1 Effect of Injection Flow Rate on Stock Solution COD and BOD in LC Medium.

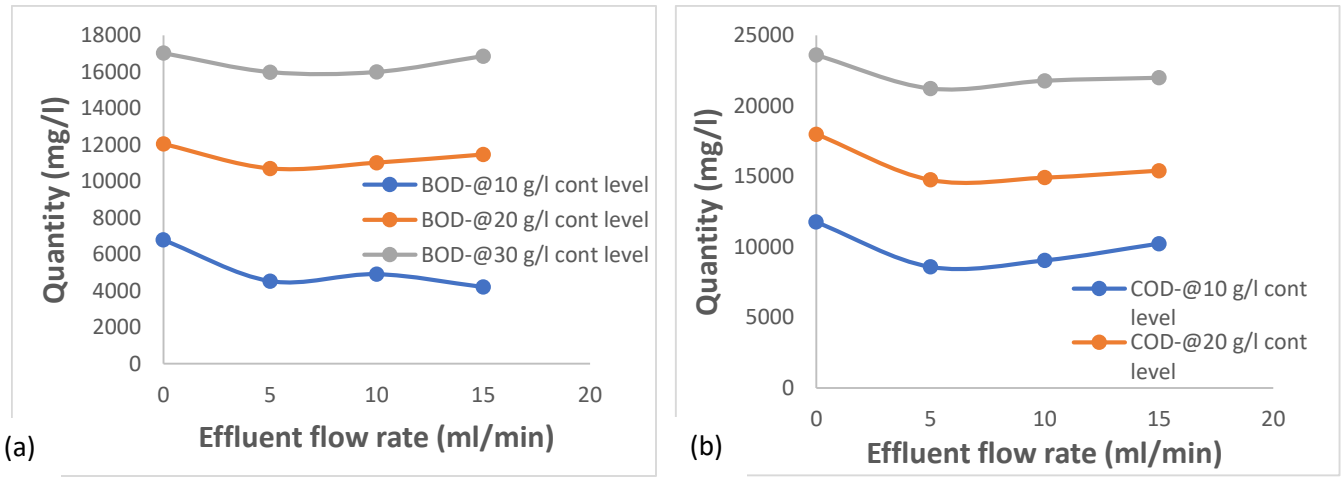

Fig. 19 (a & b): Stock solution COD and BOD behavior over LC Medium at increasing injection rate

The biological oxygen demand (BOD) of the stock solution as well as the chemical oxygen demand (COD) as physicochemical properties of the stock solution also shows a negative response to increase in the injection flow rate of the system The presents an increasing nature proportional to increase in injection rate exceeding 5ml/min and this act reduces the treatment efficiency of the LC adsorbent over time. As the flow rate increases from 5ml/min o 10ml/min and to 15 ml/min, the 10g/l concentrated stock solution shows a BOD reduces from 6778 mg/l to 4535 mg/l at the 5ml/min before experiencing a sudden increase to 4911 mg/l and 4209 mg/l proportional to increase in injection flow rate from 5ml/min to 10ml/min and 15ml/min respectively, while for 20g/l a reduction from 12052 mg/l and 10706 mg/l before increasing back to 11025 mg/l and 11474 mg/l proportional to increase in injection flow rate from to 10ml/min and 15ml/min respectively. Also, the 30g/l concentrated solution experiences an increase of the BOD from 15996 mg/l to

16002 mg/l and 16872 mg/l respectively to increase in the injection flow rate from 5ml/min to 10ml/min and 15ml/min. BOD behavior under increase in injection flow rate is similar to that of the COD as seen at Figure 19, but COD tends to be more stable in its behavioral change as well as more responsive, especially for the 10g/l concentrated BOD behavior.

Effect of Injection Rate on Stock Solution Ni, Cu and Zn amount in LC Medium

In assessment of the Ni-Cu-Zn metal ions behavior in the system as a function of injection flow rate, it was identified that the metals concentration in the stock solution reduces with increase in the injection flow rate as 5ml/min is exceeded. After the reduction in Ni^{2+} ion amount from 943 mg/l to 614mg/l at 5ml/min injection rate, suddenly the amount increases back to 689 mg/l and 722 mg/l proportional to increase in the flow rate of the injected fluid from 5ml/min to 10mml/min and 15ml/min for the 10g/l concentrated stock solution fluid. While for the 20g/l concentrated solution, a reduction of 1178 mg/l Ni^{2+} ion to 954 mg/l after 5ml/min injection experiences sudden increase to 984 mg/l and 1022 mg/l over injection of rate increase to 10ml/min and 15ml/min respectively, so as well for the 30g/l concentrated stock solution as seen at Figure 20 after been reduced from 1626 mg/l to 1554 mg/l within 5ml/min injection rate, experiences an increase to 1577 mg/l and 1610 mg/l proportional to increase in the flow rate. Same as experienced by the Cu^{2+} ion is applicable to Zn^{2+} and Cu^{2+} metal ions, but among the three metals, Cu^{2+} tends to be of high response to the change or increase in injection flow rate. Also, it was noticed that lesser impact of the increase in injection rate on the metals adsorption amounts is experienced by highly concentrated solutions which depicts that the injection fluid rate causality reduces in magnitude with increase in the solution concentration.

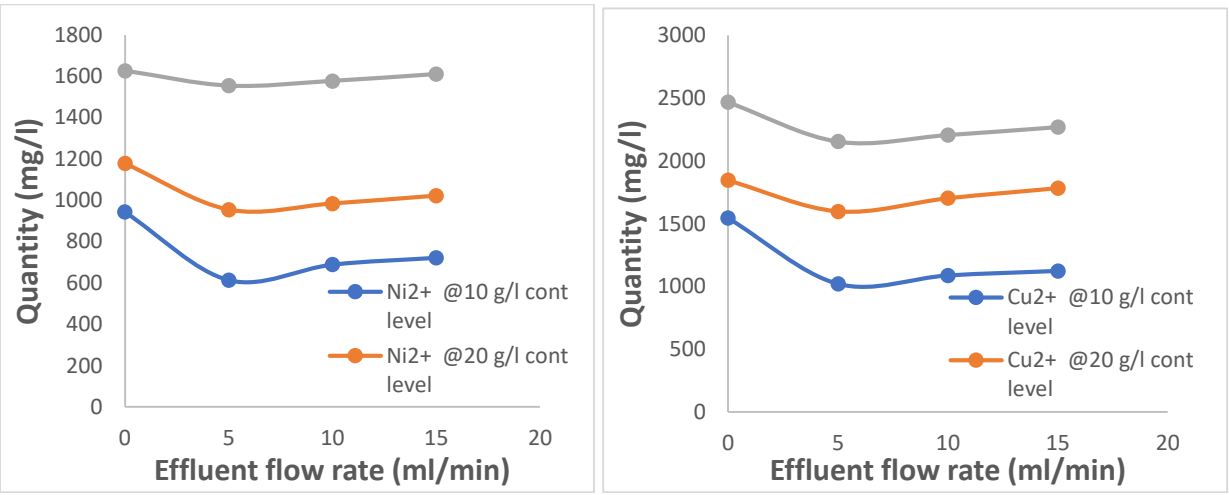

(b)

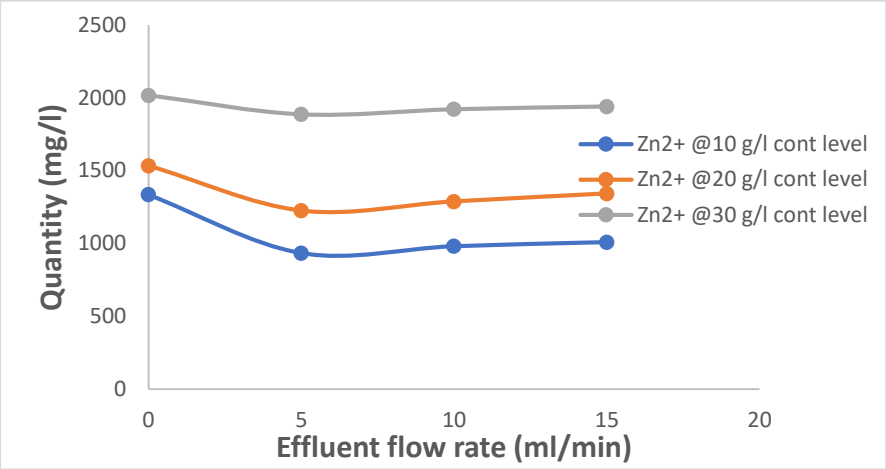

(c)

Fig. 20 (a, b and c): Stock solution COD and BOD behavior over LC Medium at increasing injection rate

Conclusively it can be deduced that the high the fluid injection flow rate into the LC-ACs loaded reactor bed, the lower the adsorbent adsorption efficiency in treatment or recovery of the Ni-Cu-Zn metals as well as on the reduction in the physicochemical properties of the stock effluent per time. This is quarreled to the fluidization tendency of the injected fluid of whose pressure non-stabilized the bed porosity ratio, forcing the free passage of some of the injected fluid without proper adsorption of the metals over time. This effect was realized after when the fluid injection flow rate (y) was increased above 5mL/min point.

Effect of *Luffa Cylindrica* Seed AC particulate size on Stock Solution Physicochemical and metal concentration in Aqueous Solution.

Particle size of adsorbents is also identified as an essential factor that can influence and define the nature and performance of an adsorbent when been used as a medium for treatment of gas or liquid such as the type studied in this work. The particulate size of the biosorbent scaling from 75µm to 300µm were used in this study subject to 5ml/min injection flow rate of stock solution circulated within 5cm height loaded column. The result as seen presented at Table 6 which shows that both metallic content in the effluent and the physicochemical nature of the solution are affected with changes in the adsorbent particulate size.

Table 6: Physicochemical ad metallic adoption efficiency of *Luffa Cylindrica* Seed ACs at different LC adsorbent particulate size (z)

Physicochemical	Untreated Stock Solution			Treated @ 75µm Biosorbent			Treated @ 150µm Biosorbent			Treated @ 300µm Biosorbent		
	Co-10g/l	Co-20g/l	Co-30g/l	Cfz1-10g/l	Cfz1-20g/l	Cfz1-30g/l	Cfz2-10g/l	Cfz2-20g/l	Cfz2-30g/l	Cfz3-10g/l	Cfz3-20g/l	Cfz3-30g/l
pH	4.6	3.4	2.9	5.3	4.0	3.4	4.9	4.2	3.4	4.7	4.0	3.2
TDS (mg/l)	16342	22331	31322	14704	20188	28431	15753	21100	29221	16125	21522	30863
DO (mg/l)	0.063	0.011	0.009	0.168	0.072	0.019	0.121	0.054	0.014	0.107	0.032	0.009
BOD (mg/l)	6778	12052	17033	4535	10706	15996	4979	11679	17012	5132	12005	17021
EC S/m	1333	3432	5224	701	3020	4357	865	3241	4843	1123	3308	4987
COD (mg/l)	11757	17990	23609	8586	14753	21234	9109	15322	23774	11094	15844	22028
Ni^{2+} (mg/l)	943	1178	1626	614	954	1554	691	1053	1577	890	1099	1622
Cu^{2+} (mg/l)	1543	1845	2467	1020	1597	2153	1233	1764	2278	1332	1798	2311
Zn^{2+} (mg/l)	1334	1534	2017	934	1225	1886	1043	1321	1976	1231	1443	2015

Effect of LC Adsorbent Particulate Size on Stock Solution pH in LC medium.

The pH of the stock solution shows similar behavior when compared to that experienced when it was earlier assessed on the bases of injection fluid rate. The pH tends to increase from 4.6 to 5.3 within the premises of 75 µm, then as the size of the *L.Cylindra* biosorbent was increased to 150 µm as well as to 300 µm, the pH of the stock solution happens to reduce spontaneously with respect to the increase in the adsorbent particulate size to 4.9 and 4.7 respectively as for a 10g/l concentrated injected solution. While the 20g/l concentrated injected fluid shows that the solution whose pH was 3.4 increases to 4.0 after passing through a 5cm height loaded 75 µm particulates of *L.Cylindra*, after which the pH value reduces gradually but spontaneously as experienced when 10g/l concentrated solution was assessed, to 3.9 using 150 µm and 3.5 when 300 µm was used.

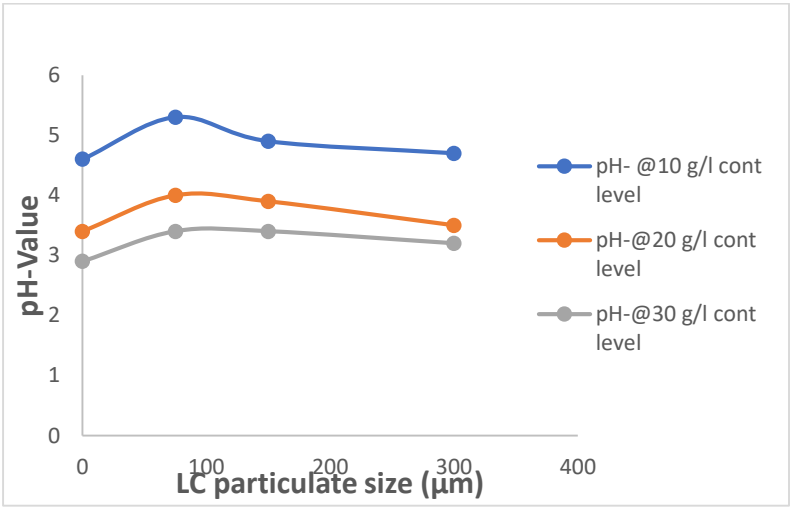

Fig. 21: Nature of stock solution pH under changes in LC adsorbent particulate size

Then for the 30g/l concentrated fluid, an increase in the pH value from 2.9 to 3.4 as the 75 µm was used was recorded, then as the LC particulate size were increased the pH also reduces as experienced with other

concentrated fluids to 3.4 and 3.2 respectively. This effect is queried to the actions of diffusivity which is known to be a key factor of adsorbtion and which is driven by the size of the permeable membrane

Effect of LC Adsorbent Particulate Size on Stock Solution TDS in LC medium.
On the stand of the injected fluid TDS, increase in the particulate size of the adsorbent above 75 µm promotes only slight reduction in the solution TDS. Base on the behavior of the 10g/l concentrated fluid, it was noticed that the effluent TDS reduces drastically from 16342 mg/l to 14704 mg/l when 75 µm was used, after which the TDS increase back to 15753 mg/l and 16125 mg/l as the size of the *L.Cylindria* biosobent particles were later increased to 150 µm and 300 µm respectively.

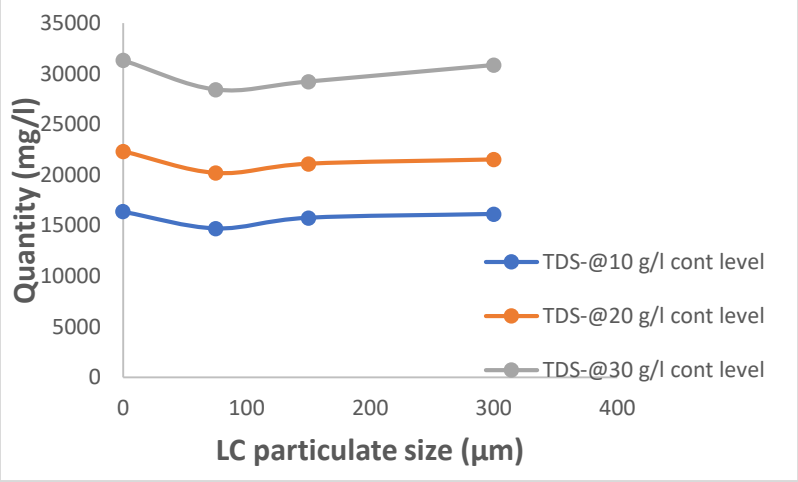

Fig. 22: Nature of stock solution TDS under changes in LC adsorbent particulate size

Similarly, effects were experienced for the higher concentrated stock solutions as seen at Figure 22, but the highly concentrated fluids tend to show more response to the phenomenon. But in all, it can be deduced that increase in the *L.Cylindrica* adsorbent size reduces the degree of TDS with the system influences to the WHO setpoint

Effect of LC Adsorbent Particulate Size on Stock Solution DO in LC medium.
The dissolved oxygen (DO) of the stock solution assessed behaves similarly to the fluid pH, such that after sudden increase as 75µm was been used, the DO reduces drastically proportional to increase in the adsorbent particulate size as seen at Figure 23. The 10g/l concentrated solution tends to first increase in its DO level from initial (0.063 mg/l) to 0.168 mg/l as 75 µm was used, then falls to 0.121 mg/l and to 0.107 mg/l as the adsorbent sizes increases to 150 µm and 300 µm respectively. While the 20g/l also increases to 0.072 mg/l from 0.011 mg/l as the 75 µm was used before showing a depletion in DO value to 0.054 mg/l and 0.032 mg/l for a 150 µm and 300 µm *L.Cylindrica* particulate sizes respectively.

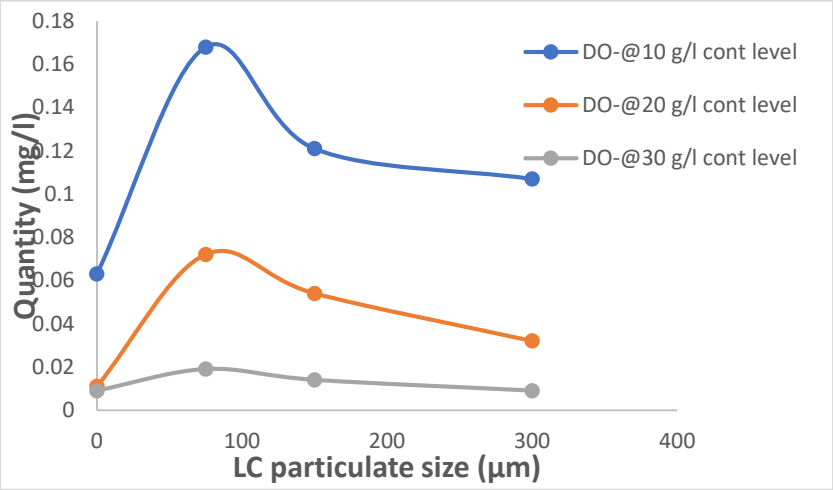

Fig. 23: Nature of stock solution DO under changes in LC adsorbent particulate size

As seen at Figure 23, the higher concentrated solution (with concentration of 30g/l) shows the highest DO response with the highest altitude The Figure 4.22 result presents the level of DO deviation from WHO setpoint as a function of concentration of the fluid ride within the regime of the adsorbent particulate size. Hence, the higher the concentration, the lower the DO balancing efficiency of LC adsorbent proportional to increase in the adsorbent particulate size.

Effect of Adsorbent Particulate Size on Solution COD and BOD in LC Medium.

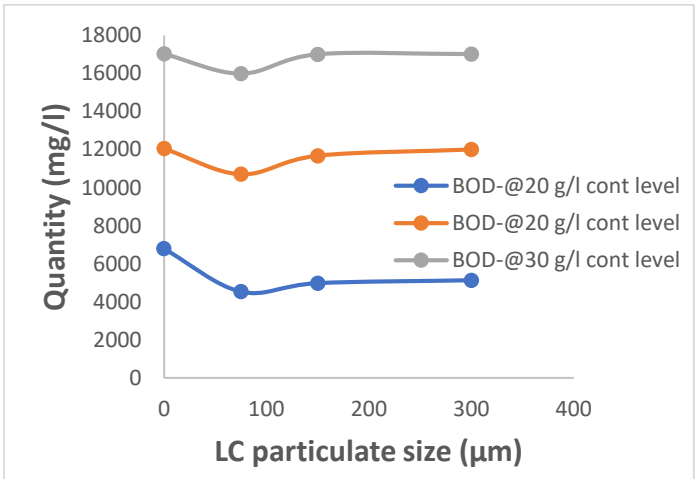

(a)

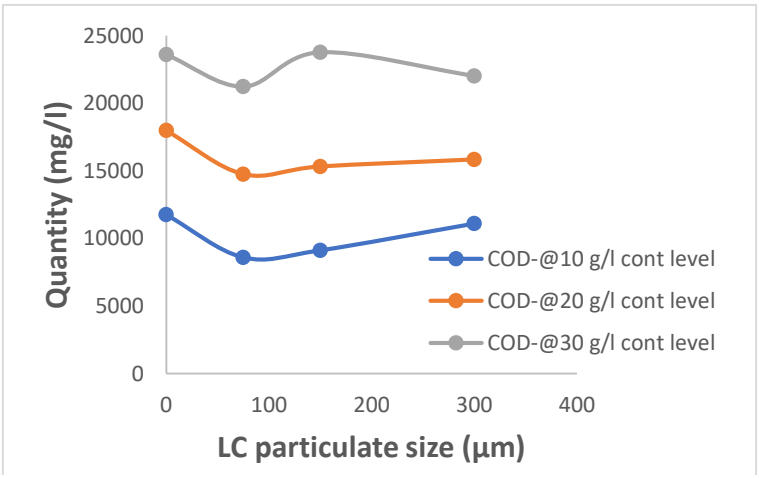

(b)

Fig. 24 (a and b): Stock solution COD and behavior over LC Medium at Adsorbent Particuiate Size.

COD and BOD also shows are negative behavior proportional to increase in LC particulate size size, such that the above 75um the COD and BOD of the stock as seen at Figure 24 turn a face from decreasing to continual increase rate. The BOD shows to be mostly affected by increase in the adsorbent particulate size when lower concentrated stock solutions are involved, while the opposite stands as the case.

Among the two physicochemical properties, COD proves to have a fast retarding nature to increasing effects of particle size increase.

Effect of Adsorbent Particulate Size on Stock Solution Ni, Cu and Zn amount in LC Medium

In assessment of the Ni-Cu-Zn metal ions behavior in the system as a function of adsorbent particulate size, it was identified that the metals concentration in the stock solution reduces with increase in the particulate size, especially the sizes above 75.

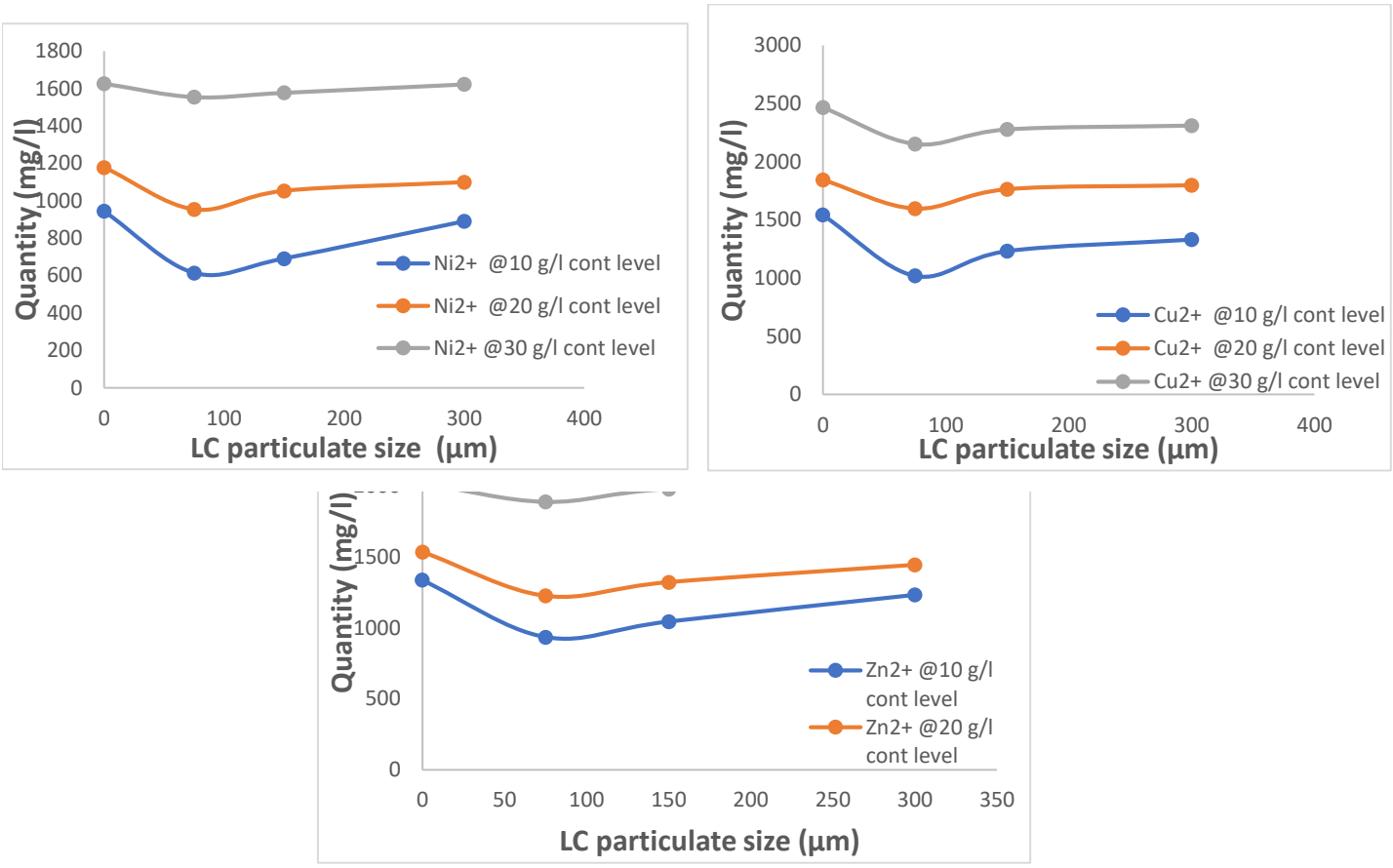

Fig. 25 (a, b and c): Stock solution COD and BOD behavior over LC Medium at increasing injection rate

Conclusively, it can be said that increase in particulate size of the LC activated carbon presents a system that depicts a reduction in the solid particulates displacement effects caused via increase in the reactor bed fluidization which is factored by increase in the fluid injection pressure or flow rate, hence promotes lesser adsorption efficiency proportional to increase in
the size of the LC particles.

CONCLUSION

LC adsorbent has proven to be very efficient in recovery of solid metals of an effluent, especially with higher reactor loading height and minimal injection flow rate.

Reference

Angon, P. B., Islam, M. S., Kc, S., Das, A., Anjum, N., Poudel, A., & Suchi, S. A. (2024). Sources, effects and present perspectives of heavy metals contamination: Soil, plants and human food chain. *Heliyon*, *10*(7), e28357. https://doi.org/10.1016/j.heliyon.2024.e28357

Ali, S., Ullah, S., Umar, H., Saghir, A., Nasir, S., Aslam, Z., M. Jabbar, H., ul Aabdeen, Z., & Zain, R. (2022). Effects of Heavy Metals on Soil Properties and their Biological Remediation, *Ind. J. Pure App. Biosci. 1*0(1), 40-46. doi: http://dx.doi.org/10.18782/2582-2845.8856

Abdel-Ghani, N. T. Hefny, M. & El-Chaghaby, G. A. F. (2007). Removal of lead from aqueous solution using low cost abundantly available adsorbents. International *Journal of Environmental Science and Technology,* 4 (1), 67-73.

Abdel-Ghani, N.T., Ahmad K. H., El-Chaghaby, G.A. & Lima, E.C. (2009). Factorial experimental design for biosorption of iron and zinc using Typha domingensis phytomass. *Desalination 249:* 343–347.

Ademiluyi, F.T. & Ujile, A.A (2013) Kinetics of batch adsorption of iron 11 I Ions from aqueous solution using activated carbon from Nigerian bamboo, international *Journal of Engineering* Technology, 3 : 623-63

Al-Auber, M. A. (2011). Thermodynamics Approach in the Adsorption of Heavy Metals, Thermodynamics Interaction Studies - Solids Liquids and Gases, PirajAin, J.C.M. (Edition.). www.intech open.com (accessed online 1st March, 2020)

Albadarin AB, Mangwandi C, Al-Muhtaseb AH, Walker GM, Allen SJ, & Ahmad MNM (2012) Modelling and fixed bed column adsorption of Cr (VI) onto orthophosphoric acid-activated lignin. Chin *Journal of Chemical Engineer* 20(3):469–477.

Al-Essa K. & Khalili F (2018) Heavy metals adsorption from aqueous solutions onto unmodified and modified jordanian kaolinite clay: batch and column techniques. *America Journal of Applied Chemistry* 6(1):25–34.

Ali I (2018) Microwave assisted economic synthesis of multi walled carbon nanotubes for arsenic species removal in water: batch and column operations. *Journal of Molecular Liquid* 271:677–685.

Babel, S., & Kurniawan, T. A. (2003). Low-cost adsorbents for heavy metals uptake from contaminated water: a review, *Journal of Hazardous Materials.* 97, 219–243.

Badmus, M.O.A. (2009). Batch studies on the treatment of brewery wastewater using charred periwinkle (*Typanotonus fuscatus*) shells. Ph.D. thesis, University of Benin, Benin City, Nigeria.

Bai, R. S. & Abraham, T. E., (2001). Biosorption of Cr (VI) from aqueous solution by *Rhizopus nigricans*. Bioresources. Technology, 79, 73-81.

Bal K. J., Hari B. K. C., Radha K., Ghale G. M., Bhuwon R.S., & Madhusudan P.U. (2004) Descriptors for Sponge Gourd [*Luffa cylindrica* (L.) Roem.], NARC, LIBIRD & IPGRI.

Basil JL, Ev RR, Milcharek CD, Martins LC, Pavan FA, dos Santos, Jr. AA, Dias SLP, Dupont J, Noreña CPZ, & Lima EC (2006). Statistical Design of Experiments as a tool for optimizing the batch conditions to Cr (VI) biosorption on *Araucaria angustifolia* wastes. *Journal Hazardous Materials*; 133: 143-153.

Bernal, V., Erto, A., Giraldo, L. & Moreno – Pirajan, J. (2017). Effect of Solution pH on the Adsorption of Paracetamol on Chemically Modified Activated Carbons Molecules. 22: 1- 14.

Dabrowski, A. (2001). Adsorption - from theory to practice. Advances in Colloid and Interface Science. 93, 135-224.

Benedict Ushaka Ugi, Mbang Obeten, Victoria Bassey, Ekerete BoEkom, Evaristus Omaliko, Frederick Ugi, Ikama Uwah (2021). Quantum and Electrochemical Studies of Corrosion Inhibition Impact on Industrial Structural Steel (E410) by Expired Amiloride Drug in 0.5 M Solutions of HCl, H2SO4 and NaHCO3. *Moroccan Journal of Chemistry*, Vol. 9, No. 4, Pp. 677-696 Index in Scopus and Clarivate analytics DOI:https://doi.org/10.48317/IMIST.PRSM/morjchem-v9i3.22346

Benedict U. Ugi (2024) Inhibition of Acid Descaling and Pickling Effects on API 5CT Carbon Steel Using C24H21N5O2 Schiff Base Ligand In 1 M H2SO4 Solution. *J. Appl. Sci. Environ. Manage*., 28 (2) 393-401 February 2024

Benedict Ugi and Mbang Obeten (2019). Inhibition of Limestone (CaCO3) Concentrated Rich Water Effects On Zinc Sheets Using Crude Alkaloids and Non Alkaloid s Extracts of *Nepeta cataria* (Catnip) Plant. *International Journal of Innovative Science, Engineering and Technology, Vol. 6, No. 3, Pp. 74 - 81*

Benedict U. Ugi, and Fredrick Bekong Ugi (2023). 817M40T Mild Steel Corrosion Remediation in 0.5 M Hydrochloric Acidic Environment Using Alkaloid and Flavonoid Extracts of Salvia Officinalis. *Physical Chemistry Research*, 12(1), 121-133.

Benedict U. U., Faith S. P., V. Bassey, Fredrick Ugi (2022). Expired CYP3A Inhibitor (Ritonavir) as Potential Corrosion Mitigator Of Petroleum Product Trunk Pipeline (20cb-3) in the Oil and Gas Sector. Conference: *Chemical Society of Nigeria South-South Zonal Conference, Workshop and Exhibition* 2022, at: Asaba, Delta State.

Du Z, Jia M, & Men J (2014) Removal of cesium from aqueous solution using PAN-based ferrocyanide composite spheres: adsorption on a fixed-bed column. Application Mechanical Materials 496–500:259–263. https ://doi.org/10.4028/www.scien tific .net/amm.496-500.259

Freitas ED, Almeida HJ, Neto AFA, & Vieira MGA (2018) Continuous adsorption of silver and copper by Verde-lodo bentonite in a fixed bed flow-through column. *Journal of Cleaner Production* 171:613–621. https ://doi.org/10.1016/j.jclep ro.2017.10.036

Gupta, N., Prasad, M., Singhal, N. & Kumar, V. (2009). Modeling the Adsorption Kinetics of Divalent Metal Ions onto Pyrophyllite Using the Integral Method. *Industrial Engineering. Chemical. Resources*, 48 (4), 2125-2128.

He J, Cui A, Ni F, Deng S, Shen F, & Yang G (2018) A novel 3D yttrium based-graphene oxide-sodium alginate hydrogel for remarkable adsorption of fluoride from water. *Journal of Colloid Interface Science* 531:37–46. https ://doi.org/10.1016/j.jcis.2018.07.017

Igwe C. I., Ugi F.B., Chikwe T. N., Gloria T. T., Ugi B. U., James B. J. (2026a) Modeling and Performance Assessment of Produced Water Injection Efficiency in Homogeneous and Heterogeneous Reservoir System as an Enhanced Oil Recovery Approach, International Journal of Petroleum and Gas Engineering Research, 9(1),81-119

Igwe C.E., Ugi F.B., Chikwe T.N., Ugi B.U., Gloria T.T. (2026b) Activated Carbon Adsorbent Porosity and Loading Factor Effects on the Adsorption Efficiency of Groundwater Treatment System for Crude Oil Hydrocarbons and Solid Metals Impurities Recovery in Niger Delta Region, *International Journal of Engineering and Advanced Technology Studies*, 14 (2), 11-54

Ita B.I., Ugi B.U., Obi D. N., Njar O. N., Adah P. U. (2026) Corrosion Inhibition of S275JR Steel in Acid Chloride using Methyltrioctylammonium Chloride and Methyltriphenyl Phosphonium Bromide - Based Deep Eutectic Solvents as Passivation Enhancers – Density Functional Theory & Molecular Simulation Analysis, Mor. J. Chem., 14(3), 1005-1024. https://doi.org/10.48317.IMIST.PRSM/morjchem-v14i3.66869

Klen, M.R.F., Ferri, P., Martins, T.D., Tavares, C.R.G. & Silva, E.A. (2007) Equilibrium study of the binary mixture of cadmium–zinc ions biosorption by the *Sargassum filipendula* species using adsorption isotherms models and neural network, *Biochemical Engineering Journal*. 34,136–146.

Lee, S. (2001). Adsorption: Theory, Modelling and Analysis. Edited by Jozsef Toth. In: Surfactant Science series. Marcel Dekker, Inc. New York, 107, 537- 572.

Lee, S, & Yoo, J. G. (2006). Method for preparing transformed *Luffa cylindrica* Roem. World Intellectual Property Organization, (WO/2006/019205).

Luqman, C. A., Muhammad, Saidatul S. J. & Thomas S. Y. C. (2010). Modelling of Single and Binary Adsorptions of Heavy metals onto Activated carbon- Equilibrium studies. Pertanika *Journal of Science and Technology* 18(1): 83-93.

Lambert M. N., Ugi F. B., Wordu A. A., Ehirim E. O., Gloria T. T., Ugi B.U., Nathaniel, O. O.7, James B. J., Oba I. (2026) Mathematical Modeling and Process Simulation of Packed Bed Reactor for Methanol Synthesis from Carbon Dioxide Hydrogenation, International Journal of Engineering and Advanced Technology Studies,14 (1), 64-97

Mandal, S., Sahu, M. & Patel, R. (2013). Adsorption Studies of Arsenic (III) Removal from Water by Zirconium Polyacrylamide Hybrid Material (Zr PACM - 43). *Water Resources and Industry*, Elsevier. 4: 51 - 67.

Martins, B.L., Cruz, C.C.V., Luna, A.S. & Henriques, C.A. (2006). Sorption and desorption of Pb^{2+} ions by dead *Sargassum* sp. biomass, *Biochemical Engineering Journal*. 27, 310 -314.

Mazali I.O., & Alves O.L. (2005). Morphosynthesis: high fidelity inorganic replica of the fibrous network of loofa sponge (*Luffa cylindrica*). Anais da Academia Brasileira de Ciências, 77, 1, 25-31.

Newton, A., Thunell, R. and Stott, L. (2006). Climate and hydrographic variability in the Indo-Pacific Warm Pool during the last millennium. Geophysical Research Letters 33: doi: 10.1029/2006GL027234. issn: 0094-8276.

Nathaniel, O. O., Wordu A. A., Ehirim E. O, Gloria T. T., Lambert, Miebi N. (2026) Mathematical Modeling of Fluidized Bed Reactor for CO_2 Capture in a Typical Cement Producing Plant Existing in Nigeria, International Journal of Engineering and Advanced Technology Studies,14 (1),41-63

Obeten, M. E, Ugi, B. U. and Alobi, N. O. (2017). A review on Electrochemical Properties of Choline Chloride Based Eutectic Solvent in Mineral Processing. *Journal of Applied Sciences & Environmental Management (JASEM).* Vol. 21, No. 5. Pp. 991 – 998.

Ogolo Doris Bruce, Ehirim Emmanuel O., Goodhead T. O., Ugi Fredrick B. (2026). Modeling and Kinetics of Polypropylene Plastic Wastes Depolymerization System to Propylene in Autoclave Recycling Reactor. *International Journal of Scientific Research and Management (IJSRM)*, 14(3), 67-77. DOI: 10.18535/ijsrm/v14i03.ce01

Ozdemir O, Turan M, Turan AZ, Faki A, & Engin AB (2009) Feasibility analysis of color removal from textile dyeing wastewater in a fixed-bed column system by surfactant-modified zeolite (SMZ). *Journal of Hazardous Materials* 166:647–654. https ://doi.org/10.1016/j.jhazm at.2008.11.123

Rangabhashiyam S, Nandagopal MS, Nakkeeran E, & Selvaraju N (2016) Adsorption of hexavalent chromium from synthetic and electroplating effluent on chemically modified *Swietenia mahagoni* shell in a packed bed column. Environmental Monitoring Assessment 188:411. https://doi.org/10.1007/s1066 1-016-5415-z

Rangabhashiyam S, & Selvaraju N (2015a) Efficacy of unmodified and chemically modified Swietenia mahagoni shells for the removal of hexavalent chromium from simulated wastewater. *Journal of Molecular Liquid* 209:487–497. https ://doi.org/10.1016/j.molli q.2015.06.033

Rangabhashiyam S, & Selvaraju N (2015b) Evaluation of the biosorption potential of a novel *Caryota urens* inflorescence waste biomass for the removal of hexavalent chromium from aqueous solutions. *Journal of Taiwan Institute of Chemical Engineering* 47:59–70. https ://doi.org/10.1016/j.jtice .2014.09.034

Recepoglu YK, Kabay N, Ipek IY, Arda M, Yuksel M, Yoshizuka K, & Nishihama S (2018) Packed bed column dynamic study for boron removal from geothermal brine by a chelating fiber and breakthrough curve analysis by using mathematical models. Desalination 437:1–6. https ://doi.org/10.1016/j.desal .2018.02.022

Rowell R.M., James S.H., & Jeffrey S.R. (2002). Characterization and factors effecting fibre properties, In Frollini E, Leao, AL, Mattoso LHC, (ed.), Natural polymers and agrofibres based composites. Embrapa Instrumentacao Agropecuaria, san Carlos, Brazil 115-134.

Sammy, T. D., Ehirim, E. O. & Ugi, F. B. (2023). Modeling the Effect of Temperature for Enhanced Oil Recovery (EOR) using Steam Injection Technique. Journal of Newviews in Engineering and Technology. 5(1), 22 – 31.

Ugi, F. B., Ehirim, E. O., Wordu, A. A. and Ugi, B. U. (2023). Modelling, design and kinetics of novel Fred-Ugi environmental wastes converter reactor plant for crude oil distillates, minerals and petrochemical synthesis, *International Journal Environmental Engineering*, 12(2), 159–191.

Ugi F.B., Benedict U. Ugi & Gloria T.Tamunotonye (2025). Design of Mechanically Agitated Fermenter for a Daily Ten Tons Ethanol Production from Cool Feed Biomass. ENP Engineering Science Journal, 5(1), 61-69

Ugi B. U, Bassey V. M., Ashishie P. B., Nandi D. O., and Ugi F. B. (2023) S275JR Mild Steel Corrosion Sites Deactivation in Sodium Sesquicarbonate Heavy Deposits Using Piperaquine as Alternative Inhibitor. *Portugaliae Electrochimica Acta*, 42,101-114 101 https://doi.org/10.4152/pea.2023420202

UGİ, B. U; OJİ, N. N; UGİ, F. B; UGI, D. U; TAMUNOTONYE, G. T (2026). Corrosion Inhibitor Potential of Tropical Milkweed (Asclepias Curassavica) Plant Leaf Extracts for Reinforced Bars in Chloride Concentrated Environment. J. Appl. Sci. Environ. Manage. 30 (2) 481-490

Ugi B. U., Obeten M. E., Bassey V. M., BoEkom E. J., Omaliko E. C., Ugi F. B., Uwah I. E. (2021). Quantum and Electrochemical Studies of Corrosion Inhibition Impact on Industrial Structural Steel (E410) by Expired Amiloride Drug in 0.5 M Solutions of HCl, H2SO4 and NaHCO3. *Moroccan Journal of Chemistry*, 9(4), 677-696 677

Ugi, B. U, Obeten, M. E., Bassey, V. M, Louis Hitler, Adalikwu, S. A., Omaliko, E. C., Nandi, D. O. Uwah, I. E. (2022) Adsorption and Inhibition Analysis of Aconitine and Tubocurarine Alkaloids as Eco-friendly Inhibitors of Pitting Corrosion in ASTM – A47 Low Carbon Steel in HCl Acid Environment, *Indonesian Journal of Chemistry* vol. 22 No. 1, Pp. 1 - 16 Index in Scopus and Clarivate analytics

Ugi, B. U. (2014). Alkaloid and Non Alkaloid Extracts of *Solanum melongena* Leaves as Green Corrosion Inhibitors on Carbon Steel in Alkaline Medium. *Fountain Journal of Natural and Applied Sciences* Vol. 3, No. 1 Pp. 1 – 9 http://doi.org./10.53704/fujnas.v3i1.60

Ugi, B. U. and Magu, T. O. (2017) Inhibition, Adsorption and Thermodynamic Investigation of Iron Corrosion by Green Inhibitors in Acidic Medium. *The International Journal Of Science &Technoledge*(IJST). Vol 5 No. 4 Pp. 56 – 64.www.theijst.com

Ugi B. U., E. C. Omaliko and M. E. Ikpi (2024) Artequick as Inhibitor of Anodic Site Dissolutions in ASTM-A36 Mild Steel Corrosion: Computational and Electrochemical Approach. *Portugaliae Electrochimica Acta 42(2024) 155-171*. Index in Scopus and Clarivate analytics

Ugi, B. U. & Obeten, M. E. (2019) Inhibition of localized corrosion in 2205 Duplex stainless steel by expired myambutol (ethambutol hydrochloride) drug in acid catalyzed environment. International Journal of Innovative Science and Research Technology (IJISRT). Vol. 4. No. 11, pp. 752 - 760

Ugi B. U. (2018) Thermodynamics, Kinetics and Adsorption Studies of Andrographis Paniculata as a Green and Nontoxic Corrosion Inhibitor of Commercial Structural Aluminium in 0.5 M Hydrochloric and Hydrogen Tetraoxosulphate (IV) Acid Solutions. *Arabian J. Chem. Environ. Res.* Vol.5 no. 1 pp. 15 - 31

Ugi B. U., I. E. Uwah and P. C. Okafor (2016). Sulphuric acid corrosion of mild steel in leaves extract of Cnidoscolus aconitifolius plant. *Journal of Chemical and Process Engineering*, Vol. 46. Pp. 35 – 41

Ugi, B. U. & Obeten, M. E. (2019) Inhibition of localized corrosion in 2205 Duplex stainless steel by expired myambutol (ethambutol hydrochloride) drug in acid catalyzed environment. International Journal of Innovative Science and Research Technology (IJISRT). Vol. 4. No. 11, pp. 752 - 760

Ugi, B. U. & Obeten, M. E. (2019) Investigating the Anticorrosion Potentials of Expired Nevirapine Antiretroviral as Inhibitor of Potential Crude Oil Steel in Acidic Medium. *International Research Journal of Innovations in Engineering and Technology (IRJIET). Volume 3, Issue 4, pp 44-50.*

Volesky, B. (2003) *Sorption and Biosorption*. Montreal-St. Lambert, Quebec, Canada, BV Sorbex Inc., 316 p. ISBN 0-9732983-0-8.

Wordu, A. A; Briggs, M. I . F; Ugi, Fredrick. B; Ikenyiri P (2023). Thermodynamics, Kinetics and Equilibrium Analysis of Sulphur dioxide Oxidation in a Catalytic Reactor. *Scientific Research Journal of Engineering and Computer Science*, 3(3), 42-48

Zaini H, Abubakar S, Rihayat T, & Suryani S (2018) Adsorption and kinetics study of manganese (II) in waste water using vertical column method by sugar cane bagasse. IOP Conf Ser Material Science and Engineering 334:012025. https ://doi.org/10.1088/1757-899x/334/1/01202 5